Received: 21 January 2021 | Accepted: 4 February 2021

DOI: 10.1002/ppp.2105

RESEARCH ARTICLE

WILEY

Fluvio-thermal erosion and thermal denudation in the yedoma region of northern Alaska: Revisiting the Itkillik River exposure

Yuri Shur[1] | Benjamin M. Jones[1] | Mikhail Kanevskiy[1] | Torre Jorgenson[2,1] | Melissa K. Ward Jones[1,3] | Daniel Fortier[4,1] | Eva Stephani[1] | Alexander Vasiliev[5,6]

[1]Institute of Northern Engineering, University of Alaska Fairbanks, Fairbanks, Alaska, USA

[2]Alaska Ecoscience, Fairbanks, Alaska, USA

[3]The Woodwell Research Center, Falmouth, Massachusetts, USA

[4]Geography Department, Université de Montréal, Montréal, Canada

[5]Earth Cryosphere Institute of Tyumen Scientific Center SB RAS, Tyumen, Russia

[6]Tyumen State University, Tyumen, Russia

Correspondence
Yuri Shur, Institute of Northern Engineering, University of Alaska Fairbanks, 233 Duckering Bldg., PO Box 755910 Fairbanks, AK 99775-5910.
Email: yshur@alaska.edu

Funding information
National Science Foundation (NSF), Grant/Award Numbers: OPP-1820883, ARC-1023623, OIA-1929170; National Aeronautics and Space Administration ESIP, Grant/Award Number: 80NSSC20K0491; Russian Foundation for Basic Research; National Sciences and Engineering Research Council of Canada

Abstract

Riverbank erosion in yedoma regions strongly affects landscape evolution, biogeochemical cycling, sediment transport, and organic and nutrient fluxes to the Arctic Ocean. Since 2006, we have studied the 35-m-high Itkillik River yedoma bluff in northern Alaska, whose retreat rate during 1995–2010 was up to 19 m/yr, which is among the highest rates worldwide. This study extends our previous observations of bluff evolution and shows that average bluff-top retreat rates decreased from 8.7–10.0 m/yr during 2011–2014 to 4.5–5.8 m/yr during 2015–2019, and bluff-base retreat rates for the same time period decreased from 4.7–7.5 m/yr to 1.3–1.7 m/yr, correspondingly. Bluff evolution initially involves rapid fluvio-thermal erosion at the base and block collapse, following by slowdown in river erosion and continuing thermal denudation of the retreating headwall with formation of baydzherakhs. Eventually, input of sediment and water from the headwall diminishes, vegetation develops, and slope gradually stabilizes. The step change in the fluvial–geomorphic system has resulted in a 60% decline in the volumetric mobilization of sediment and organic carbon between 2011 and 2019. Our findings stress the importance of sustained observations at key permafrost region study sites to elucidate critical information related to past and potential landscape evolution in the Arctic.

KEYWORDS
ground ice, intermediate layer, permafrost, thermal denudation, thermal erosion, yedoma

1 | TRIBUTE TO DR HUGH FRENCH

Our collaboration with Dr Hugh French started in May 1990, when he visited the Russian National Institute of Hydrogeology and Engineering Geology (VSEGINGEO), in Moscow. At that time, VSEGINGEO had one of the strongest permafrost research units in the USSR, led by Drs Stanislav Grechishchev and Eugeniy Melnikov. Dr French's enthusiasm, friendliness, and genuine interest in Russian permafrost research made communication easy and productive despite the language barriers. Evening barbecues in the nearby forest made his visit even more memorable. This visit set Dr French's regular interaction with Grechishchev, Melnikov, and some of the authors of this paper.

Our mutual research started in 2003, when Dr French joined our studies of yedoma—Late Pleistocene syngenetic permafrost with large ice wedges—in the Cold Regions Research and Engineering Laboratory (CRREL) permafrost tunnel near Fairbanks, Alaska. Permafrost in the tunnel had been studied for more than 30 years before our research, mainly by geologists and engineers[1,2] and some permafrost issues, such as cryostratigraphy, had been overlooked and the genesis of some massive-ice bodies misinterpreted. After 10 years of extensive yedoma studies in northern Yakutia, we recognized that original Pleistocene syngenetic permafrost (yedoma) in the main horizontal tunnel (adit) of the permafrost tunnel had been greatly affected by thermokarst and thermal erosion and only part of it was preserved in undisturbed condition. It was difficult initially to differentiate the

original syngenetic permafrost from later modifications because the soil itself was the same Fairbanks silt. To resolve the problem, we used a cryostratigraphic analysis as the main method to identify cryostructures typical of yedoma previously described elsewhere. In the tunnel, layered, lenticular–layered, and micro-lenticular cryostructures of soil were the most common, and the last is the main 'signature' one of yedoma. In contrast, reticulate cryostructure commonly indicates local thaw modification of original syngenetic permafrost.[3,4] The other important characteristic of yedoma is its high ice content, whereas the ice content of soil later modified by thaw is much lower. Using a cryostratigraphic approach, we identified original and modified permafrost in the adit. Dr Matthew Bray, then a graduate student, mapped the entire adit using cryostructures and properties of soil as indicators of original and modified yedoma.[5]

Two types of massive ice occurred in the tunnel: first, foliated ice wedges typical of yedoma; and second, horizontal bodies of clear or whitish ice up to 7 m wide and previously interpreted as buried pond ice.[1,2] The cryostratigraphic analysis of the latter ice and adjacent soils showed that the ice was secondary and enclosed in the original yedoma.[3,5–7] We interpreted the clear ice bodies in the CRREL tunnel to be thermokarst-cave ice[8,9] that forms in underground erosional channels filled with water. In North America, this type of ice was termed 'pool' ice.[10,11] We also described a previously overlooked type of permafrost cryostructure—reticulate-chaotic, which is associated with thermokarst-cave ice. Our later studies at numerous sites and modeling in the laboratory[6] verified this close association.

During our mutual work, Dr French visited Fairbanks five times and the results of our research were published in Shur, French, and Bray (2004),[3] Bray, French, and Shur (2006),[5] and Kanevskiy, French, and Shur (2008).[12] Our work with Dr French also helped to refine the principles and methods of cryostratigraphy.[4] Some findings from these studies are reflected in the fourth edition of Dr French's famous book *The Periglacial Environment*.[13] During the 9th International Conference on Permafrost (2008), Dr French shared findings of the research in the tunnel with numerous conference participants.

In 2011, Dr French visited our yedoma study site at the Itkillik River (Figure 1). He was impressed with the 35-m-high and 700-m-long yedoma exposure. Our discussions on yedoma in general, and the Itkillik River yedoma exposure in particular, included topics of several future publications and outlined their structures. Unfortunately, these plans were never realized. After this trip, we were preoccupied with other projects and Dr French was working on the fourth edition of his book. Nobody imagined that our cooperation would end so unexpectedly. Our mutual interest in ground ice and yedoma deposits, understanding the dynamic past and unlocking information that will inform future permafrost landscape research is something that Dr French's legacy has helped to shape. We are grateful for the opportunity to have collaborated with such a talented and experienced colleague.

2 | INTRODUCTION

Yedoma is a term for ice-rich syngenetic permafrost that accumulated during the Late Pleistocene within unglaciated areas of Eurasia and North America.[14–16] These silty deposits may exceed 50 m in thickness and contain large ice wedges.[17,18] In Alaska, yedoma deposits have been observed in many areas of continuous and discontinuous permafrost. In some areas, yedoma underlies only a small part of the landscape, whereas in others it is a dominant terrain unit (Figure 2). In many poorly drained areas, yedoma has been strongly reworked by thermokarst since the end of the Pleistocene, especially in the discontinuous permafrost zone. The main yedoma areas in Alaska include the 'Silt belt' in northern Alaska, Seward Peninsula and adjacent areas in northwestern Alaska, and parts of interior Alaska.[14] Yedoma also occurs in some areas of Canada unglaciated in the Late Pleistocene.[19–23]

FIGURE 1 Dr Hugh French at the Itkillik River yedoma exposure, August 2011

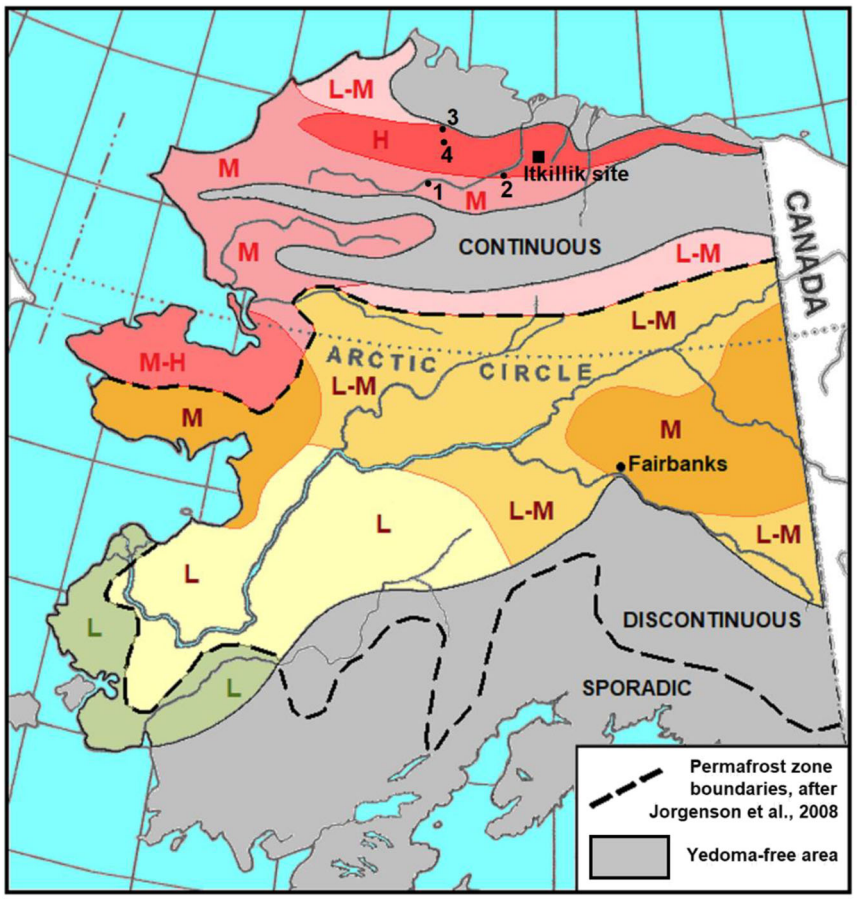

Yedoma occurrence:

	Low (L)		Medium (M)		High (H)
Continuous Permafrost		L-M	M	M-H	H
Discontinuous Permafrost	L	L-M	M		
Sporadic Permafrost	L				

FIGURE 2 Yedoma occurrence (qualitative estimate of areas occupied by yedoma deposits) in Alaska within different permafrost zones and location of the Itkillik River study site (modified from Kanevskiy et al.[14,28]). Other riverbank yedoma sites in northern Alaska mentioned in the paper: 1, 2—Colville River,[72,73] 3—Titaluk River,[26,31] and 4—Ikpikpuk River[74]

In northern Alaska, yedoma is widespread in the lower Arctic Foothills and adjacent parts of the Arctic Coastal Plain.[14,24–31] Thawing of yedoma in northern Alaska, as elsewhere, started near the end of the Pleistocene and resulted in the formation of large thermokarst-lake basins up to 20–30 m deep.[26,32,33] Within poorly drained plains, yedoma has been strongly reworked by thermokarst lakes, and in many areas undisturbed yedoma occurs mainly as relatively small remnants surrounded by drained thermokarst-lake basins. Within well-drained terrain, thermokarst-lake basins are much smaller and less common.[34] In the areas of the higher Arctic Foothills, ice-rich sediments covering bedrock are generally thin, though in some river valleys the thickness of ice-rich yedoma can reach 10–15 m.

The soil between ice wedges in the yedoma is ice-rich and thaw-susceptible. When exposed, as in a river cut bank, yedoma degrades rapidly, especially in contact with flowing water. This process, which may affect riverbanks, shores of seas, and lakes or deep gullies, is called thermal erosion. Destruction of yedoma by thermokarst and thermal erosion substantially reshapes landscapes, changes hydrologic patterns, and affects vegetation succession. It strongly affects biogeochemical cycling because yedoma soils contain large amounts of organic matter, part of which may be released to the atmosphere as greenhouse gases.[15,16,35–38] Erosional processes of all kinds result in mobilization, transport, and redeposition of organic carbon.[39–49]

Most studies of yedoma erosion relate to sea shores, whereas information on rates of riverbank erosion and volumes of reworked material is somewhat limited, but is important for estimating sediment transport and organic and nutrient fluxes into river channels and the Arctic Ocean. In the Russian Arctic, long-term rates of fluvio-thermal

erosion of yedoma riverbanks vary from 2 to 9 m/yr,[48,50–56] similar to the long-term rates of coastal erosion in the same region.[57,58] In North America, most riverbank erosion studies in permafrost regions have been performed outside of the yedoma region.[59–66] However, since 2006, we have performed permafrost studies at the Itkillik River yedoma site in northern Alaska. We reported our main results regarding riverbank erosion, including estimates of short- and long-term (years and decades, respectively) rates of fluvio-thermal erosion and thermal denudation during 1995–2011.[28]

In our previous studies at the Itkillik River site, we described the cryostratigraphy and estimated the ground-ice content of yedoma deposits.[14,28] We summarized available information on riverbank erosion in various permafrost regions, including the Itkillik River study area. We also described three main stages of riverbank evolution in the areas of ice-rich permafrost: (a) fluvio-thermal erosion combined with thermal denudation, (b) thermal denudation, and (c) slope stabilization. We found that extremely active erosion of the 35-m-high exposure along the Itkillik River started in 1995, when the river abruptly changed its course. From 1995 to 2010, the average retreat rate for the most actively eroded part of the Itkillik River bank was 19 m/yr; in 2007–2011, the average retreat rate for the whole 680-m-long bluff was estimated at 11.4 m/yr, with some parts retreating at 24 m/yr.[28]

Here, we update our observations of the processes of fluvio-thermal erosion and thermal denudation at the Itkillik River study site in the context of numerous discussions with the late Dr Hugh French at the site in 2011. We extend our previous observations from 2011 to 2019, and evaluate rates of fluvio-thermal erosion and thermal denudation of the Itkillik River bank based on newly available remote sensing data acquired between 2011 and 2019 and provided through the NGA-NSF public–private initiative: ArcticDEM.[67] Our findings highlight the linkage between fluvio-thermal erosion and thermal denudation in sustaining the rapid retreat of river bluffs and the mobilization of large volumes of sediment over decadal timescales. Our study also focuses on stabilization of yedoma slopes, including formation of baydzherakhs (tall, conical thermokarst mounds) and recovery of the ice-rich intermediate layer after termination of thermal denudation.

3 | STUDY AREA

The study area is located within the Colville River basin at the boundary of the Arctic Coastal Plain and the Arctic Foothills in northern Alaska (Figure 2). Our field study was conducted on the 35-m-high and 680-m-long vertical bluff of exposed yedoma with large syngenetic ice wedges located on the eastern bank of the Itkillik River (69°34′N, 150°52′W) (Figure 3) from August 2006 to July 2019 during five field trips.[14,28,68,69] The study area belongs to the continuous permafrost zone. Permafrost thickness in this part of northern Alaska varies from 200 to 300 m.[70] The mean annual air temperature measured at the Umiat station of the USGS Global Terrestrial Network for Permafrost, located 54 km to the southwest of the study site, was −10.2°C during 1999–2019; and the mean annual ground temperature of permafrost at 95-cm depth was −4.8°C (Frank Urban, U.S. Geological Survey, pers. comm., 2020). Warm-season precipitation during 2009–2013 at the UAF meteorological station (DUS2,

FIGURE 3 General view of the 35-m-high Itkillik River yedoma exposure. Top: August 2007 (two people stand above the bluff for scale); middle: August 2011; bottom: July 2019. Photographs taken from approximately the same location each year show the build-up of slumped material at the base of the bluff since 2011 and a transition to predominantly thermal denudation of the bluff top

Anaktuvuk River), located 17 km to the southwest of the Itkillik bluff, varied from 87 to 145 mm (112 mm average), and snow water equivalent varied from 82 to 107 mm for the same period.[71]

Our study site is not the first one described in this area. Carter[26] studied two smaller exposures that belonged to the same large remnant of continuous, flat yedoma plain. His sites 2 and 3 were located 2 and 3.5 km downstream from our site, respectively. Carter's site 2 was described as an active thermokarst amphitheater with baydzherakhs; the exposed face during the study was about 15 m high. Carter[26] interpreted the permafrost of this area as syngenetic and suggested that it may be common for the area of lower foothills, which he defined as the northern Alaska silt belt formed by eolian sediments. Several other riverbank yedoma exposures located in the central part of the silt belt have been described along the Colville River,[72,73] the Titaluk River,[26,31] and the Ikpikpuk River[74] (Figure 2).

Cryostratigraphic observations, physical properties of permafrost, and paleoclimatic and paleoenvironmental conditions at our Itkillik River study site were previously reported by Kanevskiy et al.,[14,28] Strauss et al.,[37,68] Murton et al.,[75] Lapointe Elmrabti et al.,[69] and Schirrmeister et al.[73] Generally, yedoma deposits consist of mineral solids, organic remnants of plants and animals, pore and segregated ice that form cryostructures of frozen soils, and massive wedge ice that

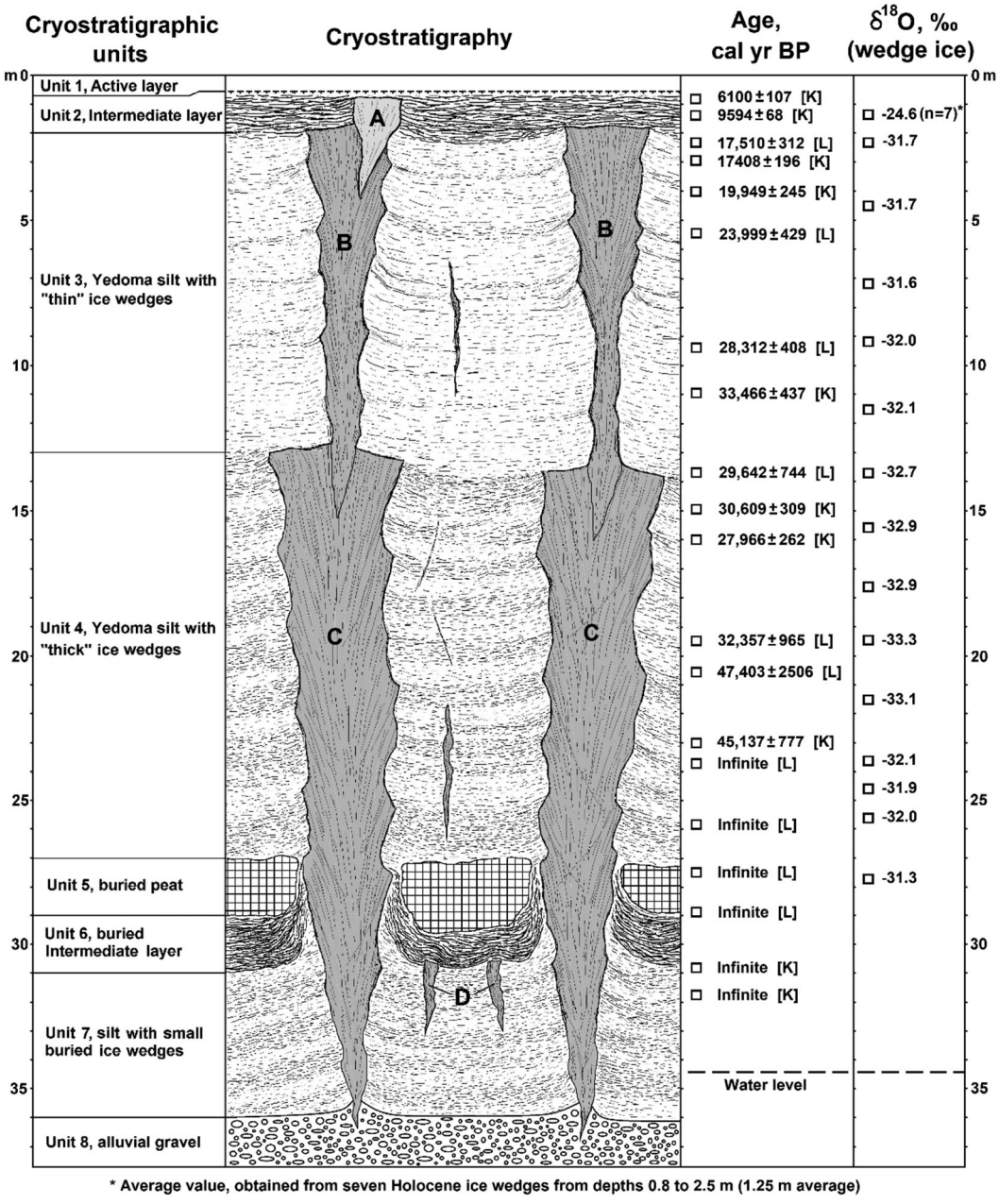

FIGURE 4 Cryostratigraphic units of the Itkillik yedoma (ice-wedge width not to scale), modified from Kanevskiy et al.,[14] radiocarbon age of deposits, cal yr BP (based on Kanevskiy et al.[14] [K] and Lapointe Elmrabti et al.[69] [L]), and stable isotope composition of wedge ice (^{18}O), ‰.[86] A, B, C, D—generations of ice wedges: A—Holocene epigenetic ice wedges of Unit 2 (Intermediate layer); B and C—Late Pleistocene syngenetic ice wedges of Units 3 and 4–7, respectively, and D—Small ice wedges of Unit 7 buried beneath the peat layer

surrounds soil columns. At the Itkillik River yedoma exposure, mineral solids of presumably eolian origin were dominated by coarse silt.[73,75] Studies of paleoclimatic and paleoenvironmental conditions of yedoma formation based on pollen data indicate the area experienced cold conditions before 35 kyr cal BP, followed by a warmer interval until 30 kyr cal BP.[69] The cryostratigraphy of permafrost at this site was previously described by Kanevskiy et al.[14,28] Currently we distinguish eight cryostratigraphic units described from the top (Figure 4), including:

0.0–0.6 m **Unit 1 – Active layer and transient layer** (a layer of soil that belongs to the permafrost for several years and joins the active layer in the years with deeper seasonal thaw[76,77]) comprising organic-rich brown-gray silt with fine sand. The combined thickness of these layers varied from 0.4 m to ~1 m depending on the thickness of surficial organic material. The gravimetric moisture content (GMC) of soil in the transient layer varied from 35 to 55%; the cryostructure was reticulate with prominent vertical ice veins.

0.6–2.0 m **Unit 2 – Intermediate layer** (a layer of ice-rich soil that forms due to a gradual decrease in the active-layer thickness because of accumulation of organic matter on the surface[4,78]) comprising ice- and organic-rich yellow-gray silt with Holocene ice wedges. This layer was dominated by ataxitic (suspended) cryostructure, and GMC commonly exceeded 100%. The thickness of the modern intermediate layer above Holocene ice wedges was up to 0.3 m, while its maximum thickness above Pleistocene wedges was up to 2 m, although at some sites affected by ice-wedge thermokarst this layer had completely degraded.

2.0–13.0 m **Unit 3 – Yedoma** comprising yellow-gray and gray uniform silt with rare small inclusions of organic matter and relatively thin syngenetic ice wedges. Soils were mainly ice-poor, with micro-porphyritic and latent micro-lenticular cryostructures (GMC 30–50%); relatively ice-rich soils with prevailing micro-braided cryostructure were observed in the upper part of the unit.

13.0–27.0 m **Unit 4 – Yedoma** comprising yellow-gray and gray uniform silt with rare small inclusions of organic matter and thick ice wedges. Cryostructures varied from micro-porphyritic and latent micro-lenticular to micro-braided and micro-ataxitic, with variable ice contents (GMC 30–100%).

27.0–29.0 m **Unit 5 – Buried peat layer** comprising dark-brown peat grading downward into ice-rich organic silt at the base of the bluff in the western and eastern parts of the exposure. In some locations, the peat formed a single layer up to 2 m thick, whereas in others this unit contained several peat layers divided by organic-rich silt.

29.0–31.0 m **Unit 6 – Buried intermediate layer** of ice-rich organic silt associated with buried peat (Unit 5). Cryostructures were mainly ataxitic with numerous ice 'belts' up to 5–7 cm thick that are typical of the intermediate layer.

31.0–36.0 m **Unit 7 – Silt** similar to units 3 and 4, with small buried ice wedges. This unit was observed in the eastern part of the exposure. The thick wedges of Unit 4 penetrated at places through this unit to below the river water level.

>36.0 m **Unit 8 – Alluvial gravel** of unknown thickness and properties. During the drilling at the bluff base in 2011, we encountered alluvial gravel at a depth of ~1.5 m below the river level but could not extract the core.

Kanevskiy et al.[14,28] described four generations of ice wedges forming different polygonal networks (Figure 4). Relatively small, active Holocene ice wedges occurred within the intermediate layer of Unit 2. These epigenetic wedges, triangular in shape, were up to 2 m wide and up to 4 m tall; commonly they penetrated into the Late Pleistocene syngenetic ice wedges of Unit 3. The latter were relatively wide at the top (true width up to 5 m), and they narrowed gradually with depth. The spacing between ice wedges varied from 7 to 10 m. Ice wedges in Unit 4 were up to 10 m wide and their width remained fairly uniform with depth. Ice wedges in Unit 7, located at the bottom of the exposure beneath the peat layer, were <0.7 m wide and 2.5 to 3 m tall. The spacing between ice wedges varied from 3 to 8 m. Wedge-ice volume varied from 40 to 52% in cryostratigraphic units 2 to 3 (45% average) and from 71 to 81% in units 4 to 7 (78% average). The total volumetric content of ground ice of the Itkillik yedoma was estimated to be 86%, based on combining proportional volumes of wedge ice (61%) and soil ice content between the wedges (65%).[28]

According to our previous study, which included an analysis of aerial photographs (1948–1979) and satellite images (1974–2010), the riverbank was relatively stable until July 1995, when the Itkillik River abruptly changed its course, thus initiating fluvio-thermal erosion of the bluff.[28] The total retreat of the riverbank affected by fluvio-thermal erosion and thermal denudation for the 15-year period (1995–2010) varied from 180 to 280 m (measured at the water level), which means that the average retreat rate for the most actively eroded part of the riverbank reached 19 m/yr.

Based on GPS (global positioning system) positions of the top of the bluff, from August 2007 to August 2011 riverbank retreat varied from less than 10 m to almost 100 m. The total area of the yedoma surface lost on top of the bluff for this period was 30,880 m^2. Thus, the average retreat rate for the entire 680-m-long bluff (the length was averaged between 2007 and 2011) at the top of the bluff was 11.4 m/yr over the 4-year period. We divided the top surface of the entire exposure into five segments with different modes of riverbank degradation, and average retreat rates for these segments in 2007–2011 varied from 2.4 to 20.3 m/yr. The most actively eroded central part of the bluff (~150 m long) retreated at a rate of 16–24 m/yr (20.3 m/yr average).[28]

4 | METHODS

4.1 | Soil and ground ice

In 2019, we continued cryostratigraphic studies that had been performed in 2007, 2011 (together with Dr French), and 2012. Cryostructures were described using classifications adapted from Russian and North American literature.[4,79] In June–July 2019, 17 boreholes up to 2.4 m deep were drilled with a SIPRE corer (7.5 cm in diameter).[80] Six of them were drilled along the yedoma slope to study recovery of the ice-rich intermediate layer on stabilized slopes, and 11 boreholes were drilled from the top of the yedoma to study the cryostratigraphy of the upper permafrost and properties of the intermediate layer along the 200-m long Itkillik River Transect (IRT) established in 2011. Eighty-three samples were collected from the boreholes to determine gravimetric and volumetric moisture contents, and excess-ice content. The samples of frozen soil were weighed, oven-dried (90°C, 72 h) and then reweighed. Gravimetric moisture content (GMC) was calculated as the ratio of the mass of the ice in a sample to the mass of the dry sample.[81] Volumetric moisture content (VMC) was calculated according to the equation[82]:

$$\mathrm{VMC} = (\mathrm{GMC} * G_s/0.9)/(1 + \mathrm{GMC} * G_s/0.9)$$

where G_s is the specific gravity of solids, which varies from 1.5 for organic soils to 2.7 for mineral soils. Excess-ice content (EIC) was calculated according to the equation:

$$\mathrm{EIC} = \mathrm{EIV}/(\mathrm{TIV}/\mathrm{VMC})$$

where EIV is the volume of excess ice in the sample (determined by measuring volumes of excess water removed with a pipette after thawing of frozen samples; numbers were multiplied by 1.09 to estimate the equivalent volume of ice), and TIV is the total volume of ice in the sample. This approach allows soil samples of any shape to be processed without spending significant time and effort on volume measurements, and is accurate enough for estimating volumetric moisture content and excess-ice content. Methods of ice-content estimation are detailed in the Supporting Information (Methods S1).

4.2 | Quantification of riverbank erosion rates and volume of eroded soil

Kanevskiy et al.[28] reported decadal-scale erosion rates for the bottom and top of the riverbank based on analysis of topographic maps, aerial photographs, and satellite images available from Google Earth, the Geographic Information Network of Alaska (GINA) of the University of Alaska http://www.gina.alaska.edu/), the U.S. Geological Survey (http://earthexplorer.usgs.gov/), and with a handheld GPS unit in the field during August 2007, August 2011, and May 2012. In this paper, we extend this time series from 2011 to 2019 using orthorectified, high-resolution (2 m) satellite imagery from the DigitalGlobe Inc. constellation of satellites, as well as digital surface models (2 m) produced by the Polar Geospatial Center at the University of Minnesota.[67]

Orthorectified images and digital surface models were provided through the NGA-NSF public–private initiative ArcticDEM.[67] As delivered, the relative horizontal and vertical accuracy of the datasets varied by 6 m and 5.5 m, respectively. To account for image-to-image location and height variability, all of the imagery was horizontally and vertically referenced to the July 15, 2017 image to remove biases inherent in the DEM data. This procedure provided a time-series dataset that was horizontally registered with sub-pixel accuracy (< 2 m) and vertically aligned to the bluff-top hinterland (< 0.3 m) and the slopes of the stabilized portion of the riverbank (< 1.0 m). The base and top of the river bluff were digitized in the orthorectified imagery in a GIS using a scale of 1:500 for six individual years of imagery between 2011 and 2019. Erosion rates were determined for both the bluff base and the bluff top using the U.S. Geological Survey Digital Shoreline Analysis System (DSAS v. 5.0) tool.[83] Transects were distributed every 3 m along the bluff base and bluff top to determine the magnitude of the erosion in each setting over the variable time periods between image acquisitions. We summarized average annual erosion rates for each of the five time periods according to bluff-base and bluff-top erosion and also summarized these values according to the five sectors presented in the previous study.[28] We estimated volumetric changes using the adjusted digital surface model datasets from the ArcticDEM.[67] Volumetric change was determined, pixel by pixel, by summing the total vertical change of each 2 m × 2 m pixel for DEMs in 2011, 2014, 2017, and 2019. The assessment area for the volumetric change detection for each of the three time periods was bracketed by the bluff base at the start of a time period and the bluff top at the end of a period.

We analyzed air temperature data from the USGS Global Terrestrial Network for Permafrost (GTN-P) site at Umiat, Alaska (Gary Clow and Frank Urban, U.S. Geological Survey, pers. comm., 2020). We determined thawing degree days (TDDs) between 2007 and 2019, and annualized the data to °C/yr in accordance with the time periods dictated by the remote-sensing observations of the Itkillik River bluff. We correlated TDDs with average retreat for the entire feature, as well as the five study segments using linear regression. We also compared the annualized TDDs and bluff-top retreat data to an empirical curve developed by Aré[84] that shows the rates of thermal denudation of vertical bluffs containing ice wedges as a function of the annual sum of all the positive mean daily air temperatures (TDDs).

We calculated the Normalized Difference Thermo-erosion Index (NDTI) for five time periods from 2011 to 2019. The NDTI is based on an approach developed by Günther et al.[58,85] for assessing the relative role of thermal denudation and thermal abrasion in coastal exposures with yedoma in Siberia. For our NDTI calculations, we modified Günther's[85] equation by replacing thermal abrasion (TA) with fluvio-thermal erosion (TE):

$$\mathrm{NDTI} = (\mathrm{TD} - \mathrm{TE})/(\mathrm{TD} + \mathrm{TE}),$$

where TD is a rate of thermal denudation measured at the bluff top and TE is the rate of fluvio-thermal erosion measured at the bluff base. The NDTI can vary from +1 (thermo-denudational regime, when the bluff base is stable) to −1 (thermo-erosional regime, when the bluff top is stable). NDTI = 0 when retreat rates at the bluff top and bluff base are equal. The limitation in this approach, based on our data, is that we cannot adequately resolve thermo-erosional niche development.

5 | RESULTS

5.1 | Soils and ground ice

During 2011, 35 boreholes up to 4.1 m deep were drilled along the 200-m long IRT with the SIPRE corer to study the cryostratigraphy of the upper permafrost and monitor processes of ice-wedge degradation and stabilization.[86] Twenty-one boreholes were regularly distributed every 10 m along the transect. Wedge ice was encountered in 15 of 21 boreholes (71%). Two generations of ice wedges were identified in these boreholes: Holocene ice wedges (7/15) and Late Pleistocene ice wedges (8/15). Holocene ice wedges were encountered at depths from 58 to 94 cm (73.4 cm average). They were protected from thawing by a layer of frozen soil (including transient and intermediate layers) up to 27 cm thick (15.9 cm average) and only two wedges experienced thawing in August 2011. Late Pleistocene ice wedges were encountered at depths from 129 to 243 cm (186.9 cm average); they were protected from thawing by a layer of frozen soil (including transient and intermediate layers) 83–201 cm thick (141.6 cm average). Five more boreholes were drilled along the transect, and several more boreholes were drilled close to the yedoma exposure. In May 2012, two boreholes were drilled through the ice of thermokarst ponds that formed above degrading ice wedges (IRT-10/12 and IRT-184/12). The thicknesses of seasonally frozen soil at the bottoms of these ponds were 100 and 88 cm, respectively.

In 2019, 11 boreholes were drilled along the IRT near the boreholes drilled in 2011 to monitor ground ice changes associated with ice-wedge thermokarst. No ice wedges were degrading by early July 2019, all ice wedges were protected by at least 30 cm of frozen soil, and thicknesses of the intermediate layer above ice wedges varied from 0 to >100 cm.

Data on the gravimetric and volumetric moisture content, and excess-ice content of frozen soils from the cryostratigraphic units are

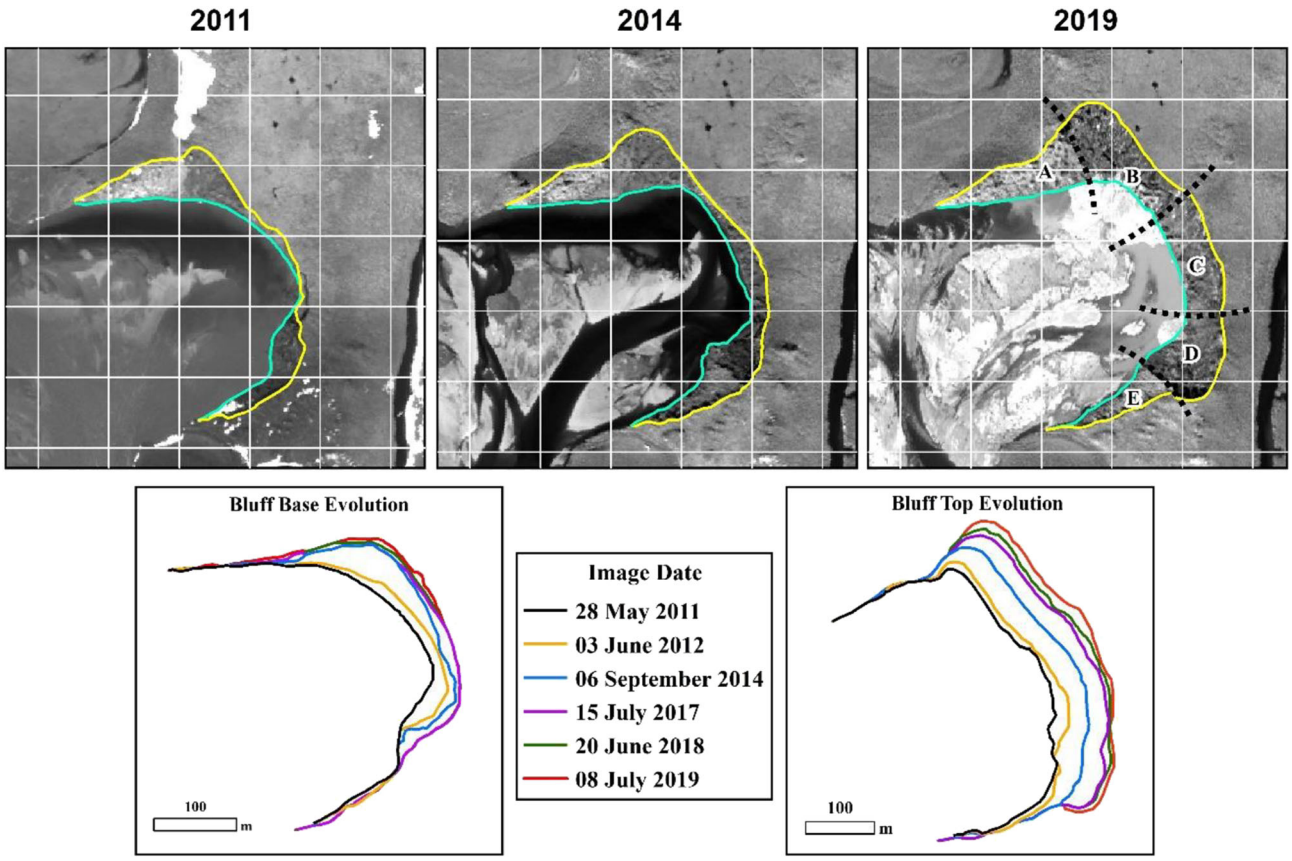

FIGURE 5 Top: high-resolution orthorectified satellite imagery from 2011, 2014, and 2019 showing changes to the bluff base (teal line) and bluff top (yellow line). The grid spacing in each image is 100 m. Five segments (A–E) with different modes of riverbank degradation are shown in the 2019 image. Bottom: sequence of digitized bluff base (left) and bluff top (right) positions showing the evolution of the feature derived from six high-resolution orthorectified satellite images between 2011 and 2019. Note that by 2019 the river channel had migrated away from the base of the bluff. Images copyright DigitalGlobe, Inc

presented in the Supporting Information (Data S1, Table S1). The average values of excess-ice content varied from 2.8% (n = 13) in the frozen part of the active layer to 8.7% (n = 9) in the transient layer and to 36.0% (n = 16) in the intermediate layer.

In 2019, we also drilled six short boreholes along a stabilized slope adjacent to the exposure (Supporting Information, Data S1, Table S2). Although small vegetated baydzherakhs still existed on some parts of the slope, we presume that this slope has been stable for centuries because it is separated from the river channel by a wide, well-developed floodplain. Soil coring revealed that in most boreholes, the thickness of reworked deposits over undisturbed yedoma exceeded 2 m, and only two boreholes on the upper part of this slope reached undisturbed yedoma. The thickness of surficial peat varied from 10 to 25 cm.

Average excess-ice contents of soils on the stabilized slope varied from 1.4% (n = 10) in the frozen part of the active layer, to 18.3% (n = 6) in the transient layer, and to 42.7% (n = 15) in the intermediate layer. Five of the six sites had a well-developed ice-rich intermediate layer 50–80 cm thick, with the average excess-ice content varying from 32 to 55% (Supporting Information, Data S1, Table S2). The borehole without an intermediate layer (IRS-5) was located near the

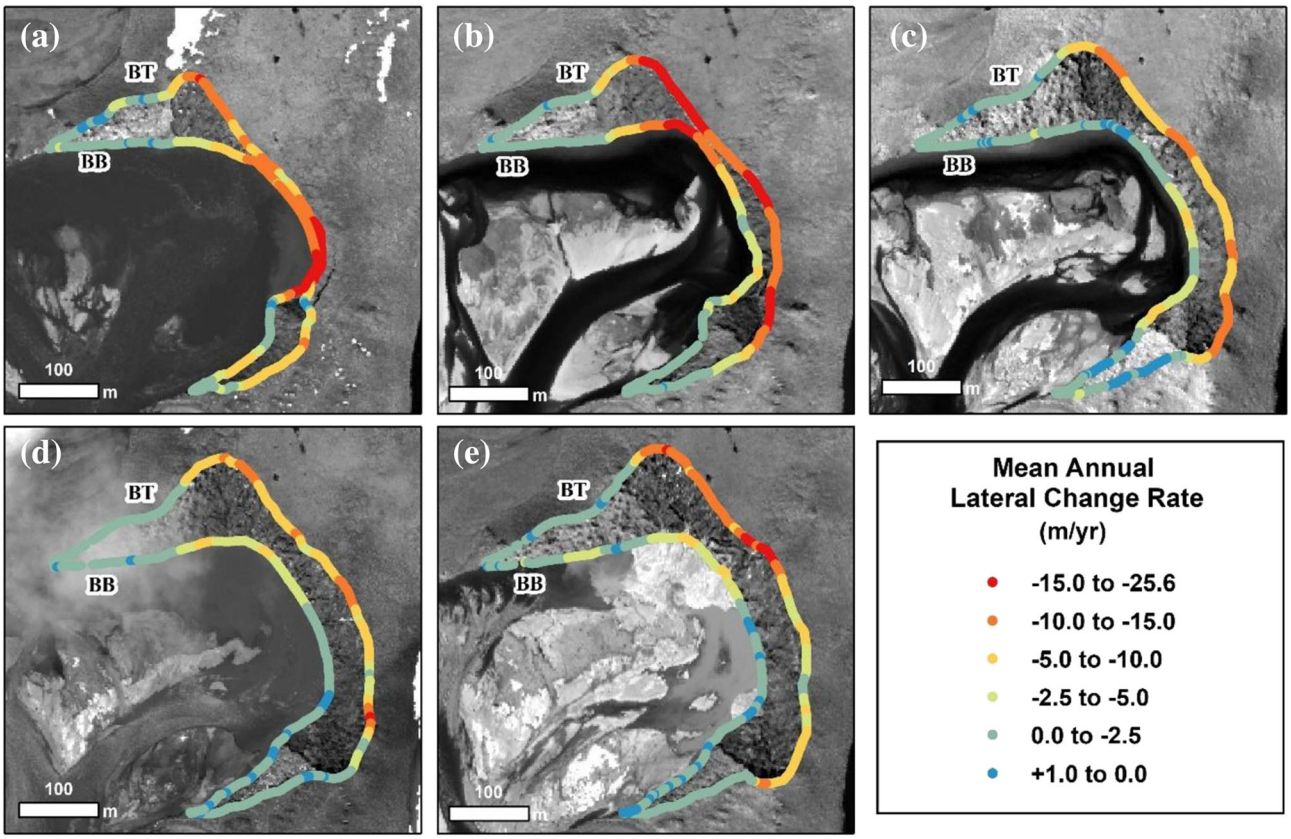

FIGURE 6 Sequence of high-resolution satellite imagery used to determine mean annual lateral change rates between 2011 and 2019. Each frame shows the rate of change at the bluff base (BB) and bluff top (BT) between two successive image pairs with the image and erosion rate points denoting the latter image date in the comparison. (a) May 28, 2011 vs. June 3, 2012, (b) June 3, 2012 vs. September 6, 2014, (c) September 6, 2014 vs. July 15, 2017, (d) July 15, 2017 vs. June 20, 2018, and (e) June 20, 2018 vs. July 8, 2019. Negative values indicate erosion. Images copyright DigitalGlobe Inc

TABLE 1 Average retreat rates of the bluff base and the bluff top between 2007 and 2019 for the entire section of the Itkillik River study site and the five segments identified in Kanevskiy et al.[28] Data from 2007 to 2011 come from Kanevskiy et al.[28]

	2007 to 2011 average retreat (m/yr)	2011 to 2019 average retreat (m/yr)	
Segment	Bluff top	Bluff top	Bluff base
A	2.4	0.8	0.8
B	11.2	10.9	6.0
C	20.3	10.3	4.6
D	17.3	9.2	4.2
E	6.4	1.5	0.8
Total	11.4	6.9	3.3

top of the slope in the small depression between two low baydzherakhs. Wedge ice in this borehole was encountered at a depth of 84 cm, which definitely exceeds the active-layer thickness at this site, so we consider this ice wedge to be relatively well protected from potential thermokarst. Undisturbed yedoma was reached at a depth of 204 cm in borehole IRS-6, situated at the upper part of the slope.

5.2 | Rates of riverbank erosion

Image analysis of the Itkillik River bluff across the entire exposure showed that erosion remained active after 2011, but at a reduced rate. Between 2011 and 2019, the average retreat rate at the bluff base was 3.3 m/yr and at the bluff top it was 6.9 m/yr (Figures 5 and 6; Table 1). Analysis of five shorter periods (1–3 years) within the 8-yr period showed that average erosion of the bluff base began to slow after 2011, decreasing from 7.5 m/yr in 2011 to 4.7 m/yr in 2012–2014, and that a step change occurred after 2015, decreasing to 1.3–1.7 m/yr between 2015 and 2019, an ~80% reduction over the 8-yr period. Average retreat rates of the bluff top increased from 8.7 m/yr in 2011 to 10.0 m/yr during 2012–2014 (Table 2). Following 2014, retreat rates of the bluff top decreased but remained quite high, averaging between 4.5 m/yr and 5.8 m/yr (~40% reduction over the 8-yr period). Maximum retreat rates of the bluff base and the bluff top also decreased during this 8-yr period, with a larger decrease occurring at the bluff base relative to the bluff top. The maximum rate of erosion at the bluff base declined from 24.6 m/yr in 2011 to 18.2 m/yr during 2012–2014, and to 6.6–8.6 m/yr during 2015–2019; by contrast, the maximum retreat rate at the bluff top declined from 25.6 m/yr in 2011 to 16.9 m/yr in 2018. We attribute the decrease in retreat rates of the bluff base to the migration of the main channel of the Itkillik River away from the exposure after 2014 (Figure 5).

Following the five segments (A–E) previously described,[28] we determined bluff-base and bluff-top retreat rates for each of our five more recent image observation periods (Table 2). Similar to the previous study,[28] segments B–D experienced the highest retreat rates of the bluff top over the 8-yr period. However, erosion of the bluff base nearly ceased in segment D following 2017, mirroring changes that began to occur in segments A and E starting between 2012 and 2014.

Bluff-top retreat rates were related to annualized TDD sums that correspond to the time periods of the remote sensing imagery using linear regression (Figure 7) to provide an indication of the magnitude of thermal denudation on bluff retreat. TDDs varied from 656 to 1,275°C/yr during the 8-yr period. Overall, no statistically significant relationships were identified between TDDs and the average retreat. However, the relationship was significant ($r^2 = 0.85$, $p < 0.05$) for the individual segment B, but not for all other segments. This suggests that only segment B was driven mostly by thermal denudation and all other segments by a combination of thermal denudation and fluvio-thermal erosion. Bluff-top retreat reached 0 m by 2014 for segment A

TABLE 2 Sequence of retreat rate measurements for the bluff base and bluff top (m/yr) and Normalized Difference Thermo-erosion Index (NDTI) for five periods between 2011 and 2019 at the Itkillik River study site. Retreat rates and NDTI values are standardized annually within each time period

	May 28, 2011 to June 3, 2012			June 3, 2012 to September 6, 2014			September 6, 2014 to July 15, 2017			July 15, 2017 to June 20, 2018			June 20, 2018 to July 8, 2019		
Segment	Bluff base	Bluff top	NDTI	Bluff base	Bluff top	NDTI	Bluff base	Bluff top	NDTI	Bluff base	Bluff top	NDTI	Bluff base	Bluff top	NDTI
A	0.7	2.2	0.5	1.0	1.8	0.3	0.5	0.0	−1.0	0.3	0.1	−0.5	1.7	0.0	−1.0
B	9.0	10.7	0.1	12.7	15.6	0.1	0.4	8.7	0.9	4.4	8.5	0.3	3.7	11.2	0.5
C	11.8	12.3	0.0	5.0	14.6	0.5	3.7	9.1	0.4	1.1	8.6	0.8	1.4	6.8	0.7
D	13.7	12.8	0.0	3.4	13.9	0.6	3.8	9.6	0.4	0.0	4.4	1.0	0.0	5.4	1.0
E	3.1	5.4	0.3	0.0	1.7	1.0	0.6	0.4	−0.2	0.0	0.0	0.0	0.1	0.0	−1.0
Total average	7.5	8.7	0.1	4.7	10.0	0.4	1.7	5.8	0.5	1.3	4.5	0.6	1.5	5.3	0.6
Maximum value	24.6	25.6	N/A	18.2	21.0	N/A	6.6	12.9	N/A	7.3	15.7	N/A	8.6	16.9	N/A

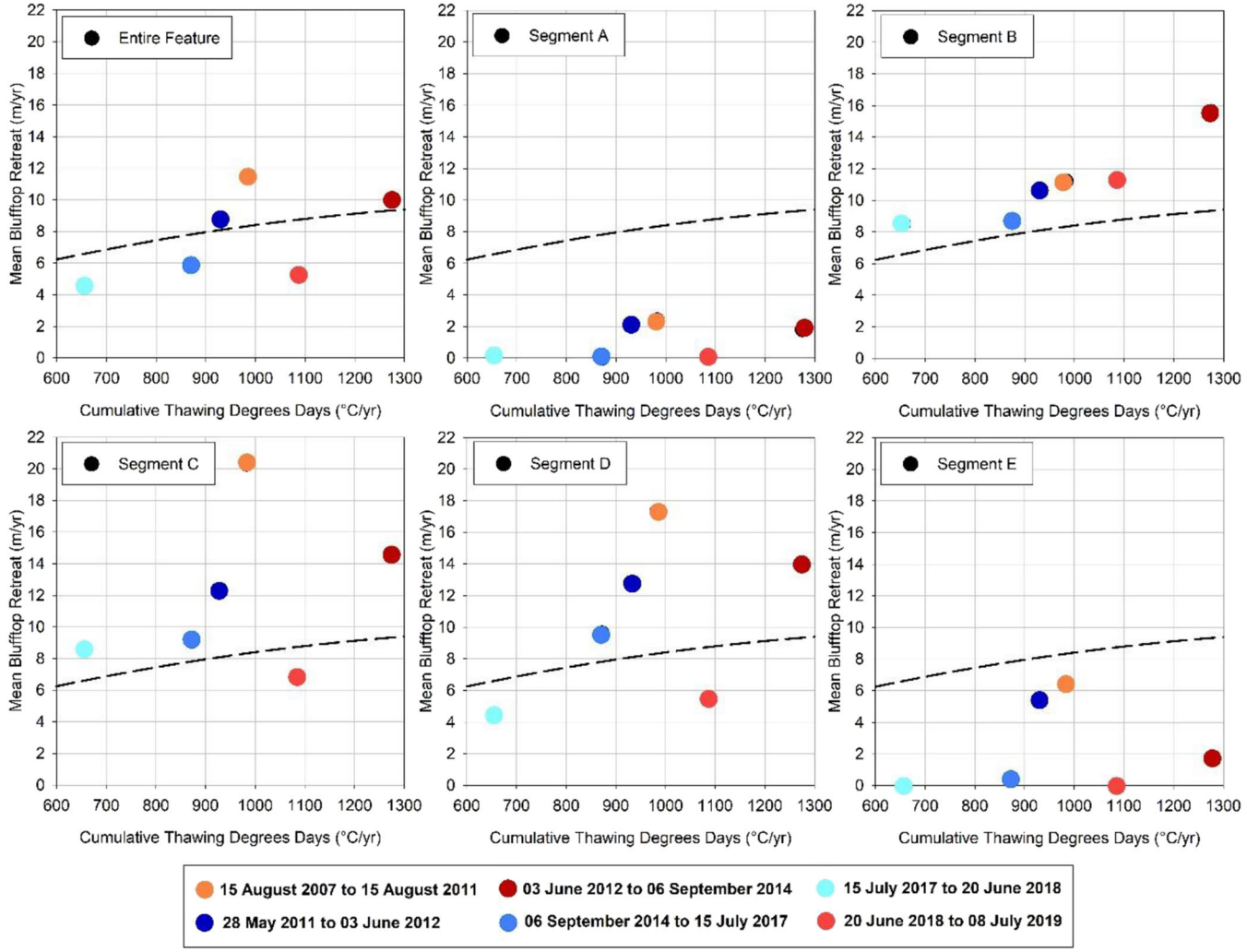

FIGURE 7 Average rate of bluff-top retreat as a function of annualized thawing degree days, as compared to the empirical curve (black dashed line) established by Aré[84] for the rates of thermal denudation of vertical coastal bluffs with exposed ice wedges in the Russian Arctic. Retreat rates from individual segments and total average bluff retreat are plotted to indicate the magnitude of thermal denudation for each annualized observation period. Segments A and E plot below the curve as these segments began to stabilize quickly. Total average bluff top retreat at segment B plots closest to the curve as thermal denudation was dominant at segment B. Segments C and D tend to plot above the curve as the combined effects of thermal denudation and fluvio-thermal erosion had a greater impact

and by 2017 for segment E, thus reaching the third stage (i.e., slope stabilization) of riverbank evolution. Although the regressions were only done with rates for the bluff top, bluff-top retreat rates depend on erosion of the bluff base as removal of material at the base will prevent sediment accumulation and slope stabilization. Thermal denudation alone accounted for half of the total average retreat for the entire bluff and was the dominant mechanism for segment B over the observation period. It was the only segment to plot above the curve based on Aré's empirical equation[84] developed for the rates of thermal denudation of vertical coastal bluffs containing exposed ice wedges in the Russian Arctic (Figure 7).

Application of the NDTI to the bluff-top and bluff-base erosion data further demonstrates the increase in the role of thermal denudation over fluvio-thermal erosion as the Itkillik exposure evolved. Between 2011 and 2012, the NDTI value was close to 0, indicating roughly equivalent forcing by fluvio-thermal erosion and thermal denudation, then increased markedly to 0.4 by 2014. After 2014, NDTI increased slightly to 0.5 and 0.6 for the remainder of the study period (Table 2).

5.3 | Topographic changes

Four of the digital surface models available from the ArcticDEM data allowed us to determine the subsidence and volumetric change of the feature over three time periods (Table 3, Figures 8 and 9). Average subsidence of the soil surface on the slope decreased from 13.0 m during 2011–2014 to 6.3 m during 2014–2017 and 3.1 m during 2017–2019. Annual rates of the total volume of eroded material decreased from 151,895 m^3/yr during 2011–2014, to 90,430 m^3/yr

TABLE 3 Results of differencing ArcticDEM digital surface models in 2011, 2014, 2017, and 2019 showing average subsidence, the planar surface area of the feature, the estimated volumetric change measured on a per-pixel basis, and the estimated annualized volumetric change at the Itkillik River study site. Volumetric changes for 2007–2011 are adopted from Kanevskiy et al.[28]

Time period	Average subsidence (m)	Planar surface area (m^2)	Estimated volumetric change (m^3)	Estimated annual volumetric change (m^3/yr)
2007 to 2011	–	–	731,520	182,880
2011 to 2014	13.0	38,318	498,192	151,913
2014 to 2017	6.3	41,017	257,840	90,232
2017 to 2019	3.1	46,365	145,224	73,315

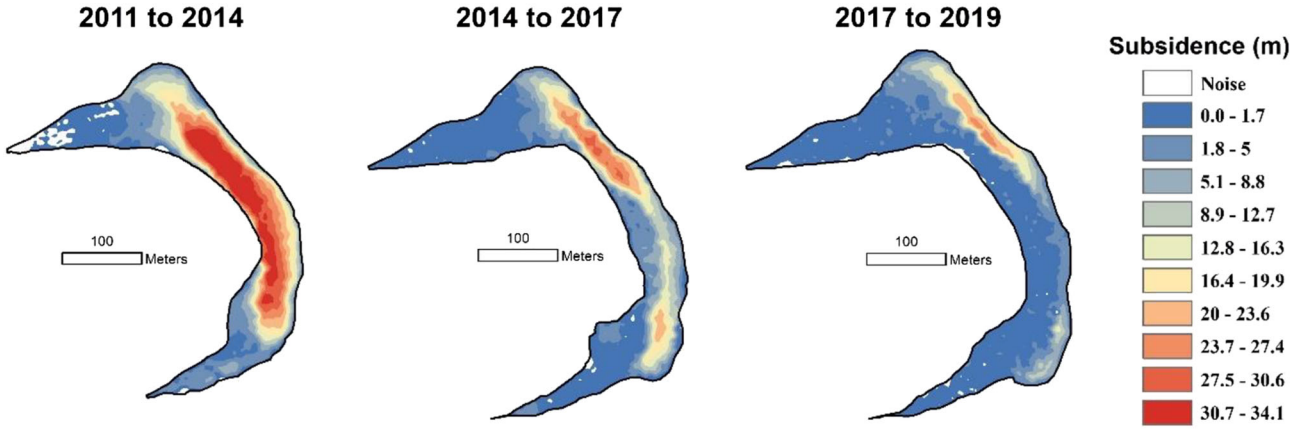

FIGURE 8 Subsidence of the soil surface measured at the Itkillik slump for three time periods between 2011 and 2019 using repeat digital surface models available from the ArcticDEM

during 2014–2017 and to 72,561 m^3/yr during 2017–2019. Taking into account the volume loss of 182,880 m^3/yr during 2007–2011,[28] the annual rates of volumetric change decreased by 17%, 40%, and 20% between each subsequent period. The very low rates of subsidence along the lower portion of the bluff compared to the high rates within the upper portion of the bluff reflect the transition from fluvio-thermal erosion to thermal denudation (Figure 8). By the 2017–2019 period, the lower portion of the bluff in segments B, C, and D had very low subsidence rates (0–1.7 m/yr), similar to those for segments A and E, indicating a shift towards stabilization (Figure 8).

Analysis of topographic profiles from representative transects from each of the five segments is an effective way to visualize the topographic evolution of changes occurring at the Itkillik exposure (Figure 9). The profile for segment A shows little to no change over time, except for minor subsidence between 2011 and 2014. The most active segment, segment B, shows that the vertical profile of the exposure was maintained throughout the time period, particularly up until 2017. Following 2017, the slope of the exposure began to relax in the lower 7–8 m, while the upper 20+ m remained vertical as a result of thermal denudation. The profiles for segments C and D follow similar trajectories; fluvio-thermal erosion and thermal denudation were very active between 2011 and 2014 and thereafter the base of the bluff began to stabilize, while thermal denudation remained somewhat active. Topographic changes at segment E resembled those at segment A, except for slightly more subsidence between 2011 and 2014.

6 | DISCUSSION

6.1 | Stages of riverbank erosion and stabilization

Based on the literature and our observations in various permafrost regions, including the Itkillik River study area, we define three main stages of riverbank evolution in areas with yedoma: (a) fluvio-thermal erosion combined with thermal denudation; (b) thermal denudation; and (c) slope stabilization.[28] Here we present a new conceptual diagram illustrating these stages of riverbank evolution (Figure 10).

During the *first stage*, fluvio-thermal erosion plays a major role. *Thermal, or fluvio-thermal erosion* refers to combined thermal and mechanical action of moving water that results in simultaneous thawing of frozen ice-bearing deposits and removal of thawed soil by water, which constantly exposes the frozen soil to further erosion.[13,28,81,87] Fluvio-thermal erosion is the most rapid process of permafrost degradation at this stage and can lead to large block failures. *Thermal denudation* is a process of thawing of frozen soils on the exposed bluff surface caused by solar radiation and convective heat exchange between the cold surface and the atmosphere, and subsequent removal of thawed soils from the bluff by mass wasting and slopewash processes.[28,84,87] Thermal denudation of high vertical bluffs with ice-rich soils and massive-ice bodies continues for years or decades after the termination of fluvio-thermal erosion.[50]

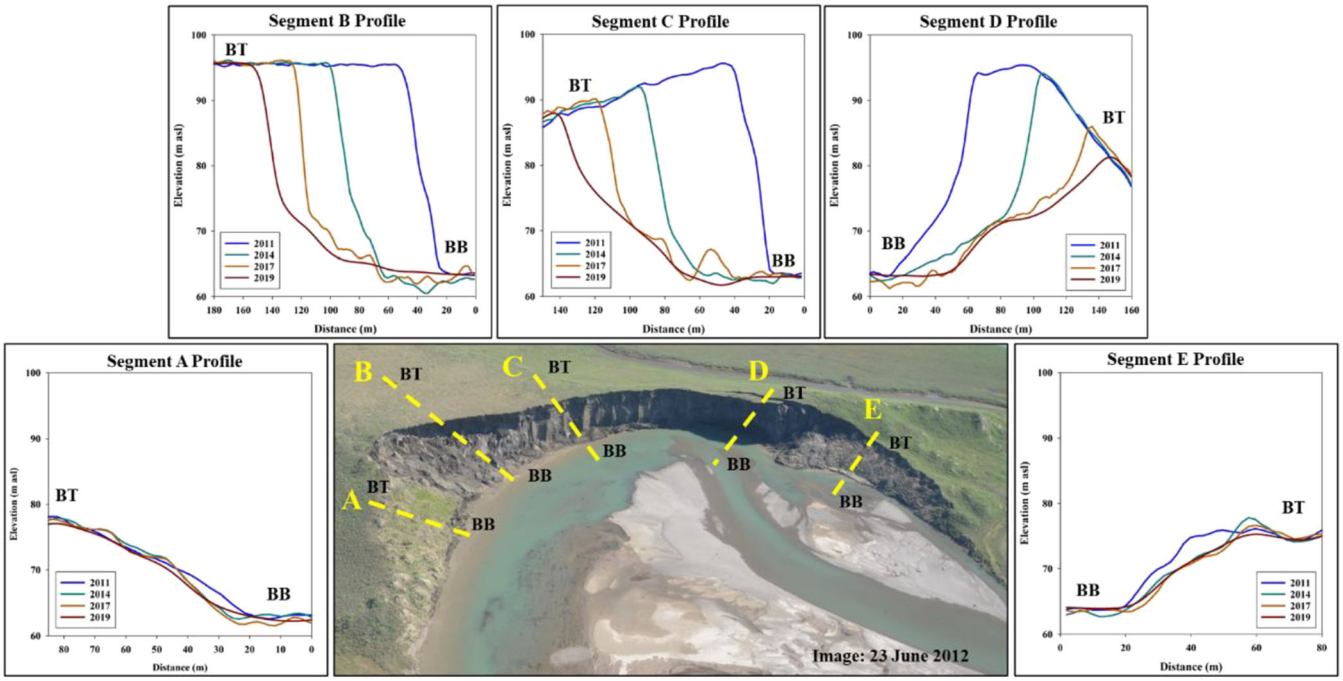

FIGURE 9 Topographic elevation profiles at the Itkillik bluff extracted from the ArcticDEM image sequence between 2011 and 2019 from representative cross-sections for segments A–E. Note that ally-axes are the same scale; the *x*-axes vary for each plot as a result of more or less erosion in a certain segment during the study period. The *x*-axes were determined based on points roughly 20 m from the bluff base (BB) in the 2011 time-step to a point roughly 20 m from the bluff top (BT) in the 2019 time-step. The photograph in the center is from June 23, 2012, during a period of rapid fluvio-thermal erosion. Beyond elevation change as a result of thermal denudation and fluvio-thermal erosion, the data probably exhibit noise associated with river-channel water, lingering snow near the bluff base in 2011, and some inherent limitations of the underlying DEM data

The first stage of riverbank erosion includes formation of thermo-erosional niches at the base of the riverbank. The horizontal depth of niches at the Itkillik site at some places was more than 10 m, and their height at openings varied from 1 to 3 m. The total lateral extent of thermo-erosional niches during our late-summer visits to the site was ~250 m in 2006, ~300 m in 2007, and less than 65 m in 2011.[28] By the time of our last visit to the study site (June 2019), the river channel adjacent to the bluff had been inactive for several years (Figure 3, bottom), and no new niches were observed.

Development of thermo-erosional niches at the base of the bluff eventually results in block falls of ice-rich soils that occur when stress on frozen soil and ice from increasing weight of frozen soil above niches overcomes the long-term strength of frozen soil or ice. Falls usually occur along ice wedges (planes of weakness) and often result in the collapse of entire polygonal blocks.[84,88] Block falls are preceded by the development of subvertical cracks above the thermo-erosional niches. In 2007, we observed several wide and deep semicircular cracks formed on the yedoma surface at distances up to 15 m from the edge of the bluff (similar cracks are visible in Figure 9, transect D). The visible depth of these subvertical cracks exceeded 10 m, and their width reached 1.5 m. Formation of these cracks resulted in a block fall that occurred on August 16, 2007 and affected more than 65 m of the bluff; the surface area at the top of the bluff was ~800 m^2 and the volume of block fall was ~15,000 m^3.[28]

Fluvio-thermal erosion is accompanied by thermal denudation of the exposed bluff above niches. During the development of niches, the part of the bluff above them retreats at a rate entirely defined by thermal denudation. Thermal denudation at this stage reduces the total rate of erosion because it reduces the size of blocks of frozen soil above niches and therefore increases the duration of time periods between block-fall events. Our observations during the period 2007–2014 best characterize this stage. We do not expect activation of the fluvio-thermal erosion in the near future because the river channel has migrated away from the bluff.

The *second stage* of riverbank erosion begins as active fluvio-thermal erosion ends and accumulation of thawed and displaced sediments (products of thermal denudation) commences at the base of the exposed bluff. At this stage, the retreat of the top of the bluff is entirely defined by thermal denudation.[28] At the beginning of this stage, the products of thermal denudation are removed by the river, so the bluff can remain vertical. When contact of running water with the exposed ice-rich permafrost no longer occurs, fluvio-thermal erosion of permafrost is replaced by mechanical erosion of thawed soil. Our observations at the site indicate that these processes maintain a rough equilibrium over several years, where the accumulation of soil at the base of the bluff (which is low because of the extremely high ice content of yedoma) balances the sediment lost to riverbank mechanical erosion.

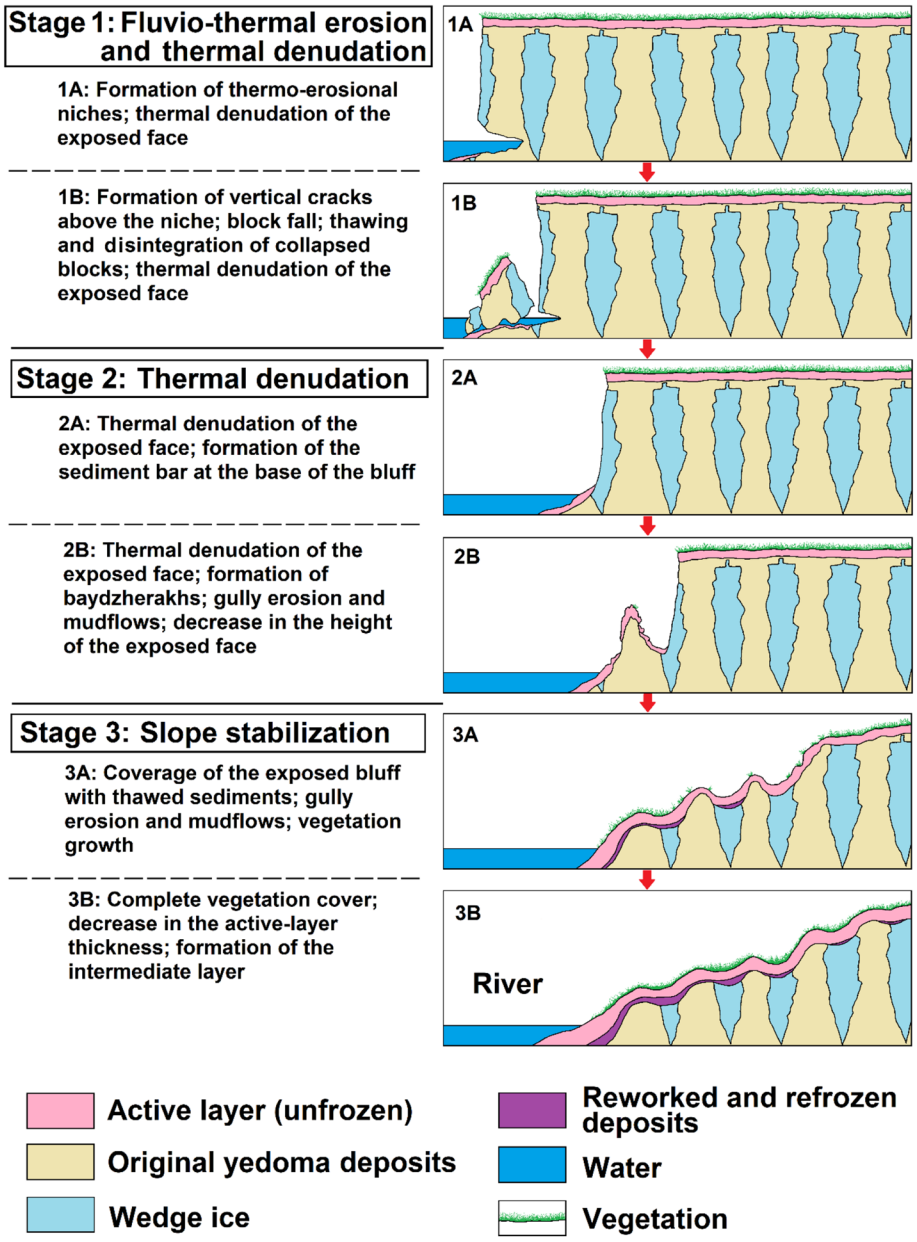

FIGURE 10 Schematic diagram showing the main stages and sub-stages of riverbank evolution in the areas of yedoma deposits and large ice wedges

Cessation of erosion activity—as occurred when the main channel of the Itkillik River shifted away from the exposure between 2014 and 2017—results in the formation of retrogressive thaw slumps with retreating vertical headwalls. The processes involved in the formation and evolution of retrogressive thaw slumps have been described in various regions of Alaska and Canada.[89–100]

Thermal denudation and continued accumulation of debris at the base of the bluff lead to significant changes in the slope profiles (Figure 9). The previously vertical bluff becomes relatively gentle in its lower part and covered with reworked sediments, while its upper part remains vertical and subject to thermal denudation. The height of this vertical exposed part decreases continually with time. This process lasts from years to decades depending on ice content, bluff height, relief behind the bluff, and climate.[50]

Active thermal denudation of the exposed vertical bluff releases meltwater, and debris-fall sediments accumulate at the base of the bluff, while the gentle lower slope is affected by numerous colluvial and fluvial processes, including slumping, mudflow, sheet and rill erosion, and gully formation (Figure 11). These processes are illustrated by a short video of the Itkillik River bluff (Supporting Information, Movie S1).

Along the vertical bluff, melting ice wedges contribute substantial meltwater, and during periods of rapid melting of the ice, the meltwater is sufficient to cause rill erosion. Thawing of ice-rich silt on the vertical bluff causes the sediment to collapse in 2- to 10-cm-thick layers, which accumulate in mounds at the base. Along the lower portion of the bluff with its 10–15° slope, the sediments move downslope through slumping and super-saturated mudflow. Downslope

FIGURE 11 Photographic examples of evidence of the processes associated with thermal denudation, which affect the bluff-face (meltwater flow and debris fall) and the lower slope (slumping, mudflow, rill erosion, linear thermal erosion), that result in the formation of the retrogressive thaw slumps with sediments eventually deposited in an alluvial fan at the river's edge

movement of the surface materials causes the overlying sediments to thin and contributes to melting of remaining wedge ice.

Melting of ice wedges on the retreating slope leads to formation of *baydzherakhs* (*thermokarst mounds*).[13,101] Baydzherakhs form due to differential thaw of wedge ice and sediment, which results in formation of residual tall conical mounds (Figures 12 and 13). These mounds are modified by slumping in the upper part and mudflows and thermal erosion in the lower part of retrogressive thaw slumps (Figure 11). The initial size and height of baydzherakhs depend on wedge-ice volume and dimensions of ice wedges. They tend to form mainly during the later phase of the overall retrogressive slump formation when thermal denudation is slower. They do not develop when slope processes are strongly active.

The *third stage* of riverbank evolution starts when the entire slope is covered with thawed and displaced soil, which leads to gradual stabilization of the slope. Transition to this stage takes many years or decades, depending on the height and ice content of the initial exposed bluff. French[13,90] concluded that the majority of retrogressive thaw slumps become stabilized within 30–50 summers after their initiation. Studies of thermal denudation in Siberia show that after the height of the exposed yedoma bluff is reduced to <4.5 m, retreat rates rapidly decrease and thermal denudation ends within several years.[50] This process, which is illustrated by the profiles presented in Figure 9, leads to transformation of the exposed subvertical bluff into a relatively gentle slope (10–15°). Continued thawing of permafrost occurs at a slow rate only in the upper part of the slope beneath a thin layer of thawed and displaced sediments. A decrease in headwall height results in decreased water and sediment input. Numerous baydzherakhs, which have formed as a result of differential thaw settlement and gully erosion during the previous stage, have partially degraded because of gravitational processes in thawed layers on the margins and summits of baydzherakhs (Figure 12). Remnants of baydzherakhs can still be visible for many decades,[78] but their height gradually decreases from soil slumping and creep.

The slope becomes practically stable when the vegetation covers its entire area. Vegetation growth and organic matter accumulation causes a decrease in the active-layer depths, an end to thermokarst, and the initial formation of an ice-rich intermediate layer.[4,28,78] We detected a well-developed ice-rich intermediate layer 50–80 cm thick in five of six boreholes drilled on a nearby thaw slump that had stabilized centuries ago (Supporting Information, Data S1). The thickness of surficial peat along this slope varied from 10 to 25 cm. In most boreholes, the thickness of reworked deposits over undisturbed yedoma exceeded 2 m, and only two boreholes on the upper part of this slope reached undisturbed yedoma.

6.2 | Rates of riverbank erosion

At the Itkillik River site, an erosion rate of nearly 20 m/yr was sustained in the central part of the bluff during 1995–2015. The comparison of retreat rates with other yedoma sites in Eurasia and North

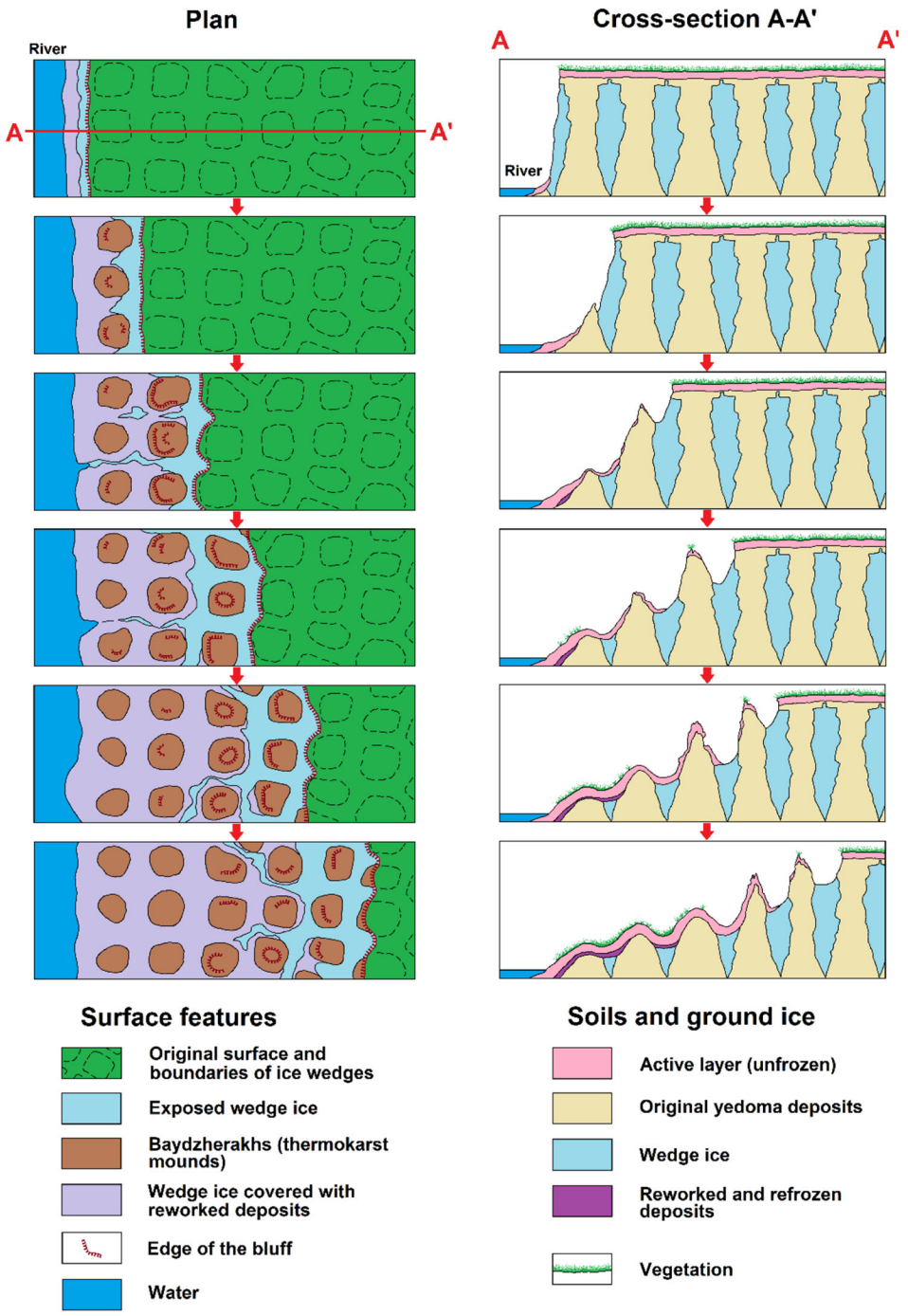

FIGURE 12 Schematic diagram showing the sequence of formation of baydzherakhs (conical thermokarst mounds) and development of retrogressive thaw slumps on steep slopes with exposed yedoma (modified from Shur and Vasiliev[101]). Reworked and refrozen sediments include both syngenetically and quasi-syngenetically frozen soils (the latter forms the intermediate layer, as vegetation growth causes the active layer to thin)

America shows that higher rates of riverbank and coastal erosion of up to 55 m/yr have been measured in Siberia for a short period (inter-annual),[102] but the long-term rates usually do not exceed 10 m/yr,[28,50,55,58,102] although at some sites they may reach 20 m/yr.[48]

Both fluvial–thermal erosion and thermal denudation are important factors affecting the high variability in erosion rates, and their relative effects can be evaluated using the NDTI.[85] To maintain high long-term erosion rates, such as at the Itkillik River site during 1995–2015, numerous block falls driven by fluvio-thermal erosion are required. NDTI values for this period of rapid erosion were close to 0, which indicates that the activity of both fluvio-thermal erosion and thermal denudation were operating equally. Our inability to detect and measure the true form of fluvio-thermal erosion and the development of thermo-erosional niches, however, probably underestimated the prominent role of fluvio-thermal erosion during this period.

By 2017, the exposed bluff at the Itkillik River site had been already separated from its base by the relatively gentle slope (Figures 6 and 9). Migration of the main channel of the Itkillik River away from the exposure between 2014 and 2017 resulted in much shorter periods of erosion activity and, therefore, reduced retreat rates at the bluff base. After 2017, erosion of the bluff base affected

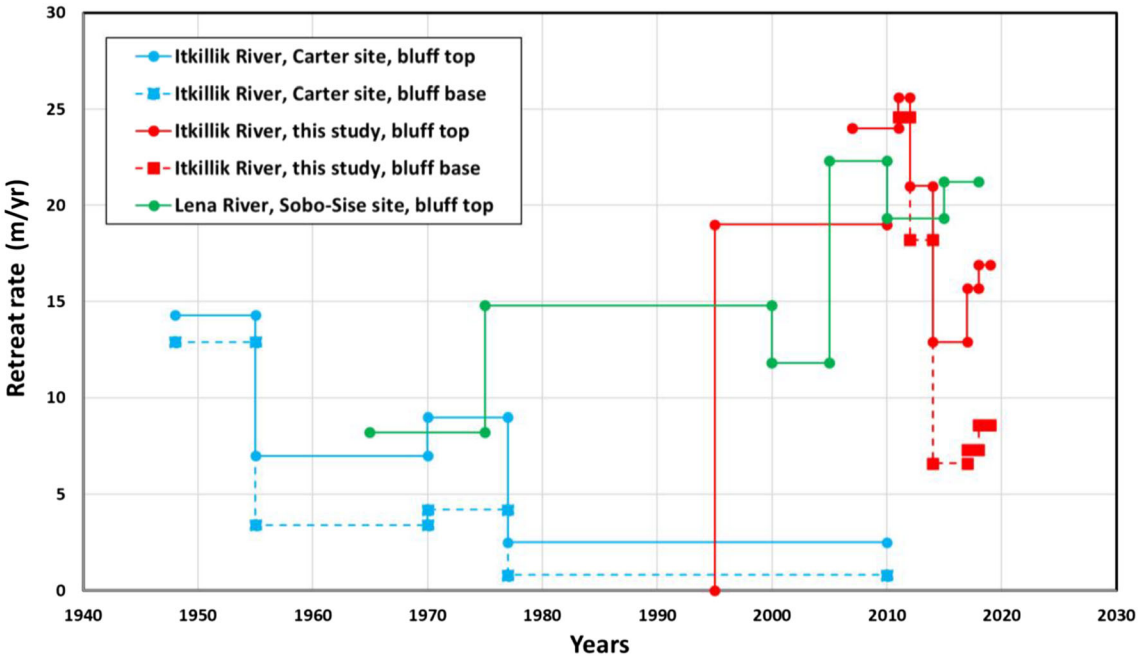

FIGURE 13 Baydzherakhs (conical thermokarst mounds) in the retrogressive thaw slump, Itkillik River yedoma exposure, July 2019

FIGURE 14 Maximum rates of bluff-top and bluff-base retreat at the Itkillik River (this study and Carter's site #2[28]) and Lena River Delta (Sobo-sise site[48])

mainly reworked sediments in the lower portion of the bluff, and it continued mainly at segment B (Table 2). This switch from combined fluvio-thermal erosion and thermal denudation to prevailing thermal denudation regime is reflected in significant increases in NDTI values from 0.1 during 2011–2012, to 0.4 during 2012–2014, to 0.5 during 2014–2017, and to 0.6 during 2017–2018 and 2018–2019 (Table 2).

The comparison of retreat rates at both the top and the base of the bluff is useful to evaluate formative processes. Comparable data are available for another Itkillik River site (Carter's site #2)[28] and for the Sobo-Sise site on the Lena River Delta, Siberia[48] (Figure 14). All these sites had very high maximum bluff-base retreat rates during some time periods: almost 15 m/yr during 1948–1955 for the Carter site; more than 20 m/yr during 2005–2018 for the Sobo-Sise site; and ~25 m/yr during 2007–2012 for our study site. Interestingly, the rates of bluff-top and bluff-base retreat for these time periods were similar for all sites. Although no data are available for the bluff-base retreat rates of the 28-m-high Sobo-Sise yedoma bluff, Fuchs et al.[48] reported that the bluff has been nearly vertical since the 2000s, which means that NDTI values during time periods with highest bluff-base retreat rates were close to 0 at all three sites.

Sharp decreases in the bluff-base retreat rates that occurred in the 1950s at the Carter site and around 2015 at our site along the Itkillik River resulted in a prevalence of thermal denudation over fluvio-thermal erosion, which is clearly visible in Figure 14. Sobo-Sise remains the only one of the three sites where fluvio-thermal erosion is still very active, which probably relates to differences in river discharge among the sites and settings. This bluff has already been degrading for more than 50 years, and during this period it experienced two abrupt increases in retreat rates during the 1970s and 2000s (Figure 14).

At the Carter site, the long-term retreat rates at the bluff top due to thermal denudation during 1948–2010 varied from 2.9 to 5.2 m/yr at different parts of the bluff. When the retreat was most active during 1948–1955, rates varied from 8.6 to 14.3 m/yr, and afterwards constantly decreased (Figure 14). When we visited this site in 2011, no frozen soils were exposed there and slope stabilization was in progress, so presumably average bluff-top retreat rates were very small. At our site, bluff-top retreat rates are still high: they reached 5.3 m/yr on average and 16.9 m/yr at maximum during 2018–2019, despite a dramatic decrease in bluff-base erosion rates (Table 2) and the height of the exposed bluff (Figure 9).

In general, the rates of thermal denudation measured at the two Itkillik River sites were similar to those at various yedoma sites in Siberia[50,52] and Alaska.[97] For example, the average retreat rate for the bluff top at the Mus-Khaya yedoma site along the Yana River in northern Yakutia was 6.5 m/yr during 1953–1989.[50] In the 1950s, it was a 40-m-high vertical bluff affected by fluvio-thermal erosion, but by the end of 1980s, after >30 years of thermal denudation, only an ~ 2-m-high vertical bluff with exposed ice-rich permafrost persisted at some places.

Our study shows that since 2011 active thermal denudation was the dominant mechanism for only one segment of the Itkillik River bluff: segment B. It was also the only segment to plot above the curve based on Aré's empirical equation[84] (Figure 7) developed for the process of thermal denudation of exposed ice wedges in the Russian Arctic. Aré's equation directly correlates retreat of a bluff with TDDs, but indirectly also includes the effect of solar radiation and moisture condensation on cold surfaces of the exposed ice-rich soil and massive ice. While acknowledging these complicating factors, we found Aré's method for evaluating average rates of thermal denudation to be roughly applicable to Arctic Alaska.

Transition from fluvio-thermal erosion to thermal denudation results in a significant decrease in the volume of eroded material. For example, the total volume of eroded material at our site decreased from ~183,000 m^3/yr during 2007–2011 to ~73,000 m^3/yr during 2017–2019 (Table 3). For the Sobo-Sise bluff (7 m lower but 2.5 times longer than the Itkillik bluff), where fluvio-thermal erosion was still very active, this volume had abruptly increased from 192,000 m^3/yr during 2000–2005 to 630,000 m^3/yr during 2005–2010, and was 581,000 m^3/yr during 2015–2018.[48]

7 | CONCLUSIONS

Extremely ice-rich yedoma is highly susceptible to riverbank and coastal erosion, with rates of bank retreat occasionally exceeding 20 m/yr. Bank retreat and the development of retrogressive thaw slumps in yedoma involves a complex interaction of fluvial, colluvial, and thermal processes that change in their relative importance over time. Fluvio-thermal erosion is the primary process that continues as long as the bluff base has direct connection with flowing river water. This process creates thermo-erosional niches that cause collapse of blocks of frozen soil and removes the eroded soil. Thermal denudation—a process of thawing of exposed ice-rich soils under the impact of solar radiation and heat exchange with air with subsequent removal of materials by mass wasting and slopewash processes—predominates once river erosion slows. Thermal denudation later interacts with sediments accumulating below the bluff that are modified by slope processes, including slumping, mudflow, sheet and rill erosion, and gully formation. Thermal denudation may act in concert or independently of fluvio-thermal erosion as exposed yedoma bluffs evolve through time. The height of the vertical bluff decreases with time, as do rates of thermal denudation. Melting of ice wedges on the retreating slope leads to formation of baydzherakhs. At later stages, thermal denudation is not only a major process leading to retreat of the bluff top but also is a mechanism of slope stabilization because it delivers material needed to transform the exposed bluff into a relatively gentle slope and protect it from fluvio-thermal erosion. Slope stabilization commonly occurs when water input from melting ice wedges becomes insufficient to cause rill and sheet erosion, as well as super-saturation of soils, and the slope angle becomes sufficiently gentle (~15°) to prevent additional removal of sediments by slumping and mudflows. Final stabilization begins when the thickness of accumulated sediments on the slope above undisturbed yedoma becomes greater than the thickness of the active layer, and vegetation

colonizes the stabilized slopes. Vegetation recovery and organic-matter accumulation lead to formation of an ice-rich intermediate layer and further burial of large ice wedges. These sequential processes eventually protect the remaining yedoma from thermokarst and thermal erosion.

ACKNOWLEDGEMENTS

The paper is dedicated to the memory of Dr Hugh French whose works and cooperation in our mutual research contributed to our knowledge of permafrost. We thank Associate Editor Julian Murton, Steven Kokelj, and Peter Morse for valuable comments that helped to improve the paper. This study was supported by the National Science Foundation (NSF) grants OPP-1820883, ARC-1023623, and OIA-1929170. D.F. acknowledges the National Sciences and Engineering Council of Canada for financial support. M.K.W.J. acknowledges support from NASA ESIP grant 80NSSC20K0491. A.V. was funded by the Russian Foundation for Basic Research (RFBR) research project 18-05-60004. We greatly appreciate CH2M HILL Polar Services for outstanding logistical support. We thank Kevin Bjella, Amy Breen, Tripp Collie, Cody Johnson, and Jens Strauss for their participation in the field work at the study site. Data are available through the NSF-funded Arctic Data Center (https://arcticdata.io/catalog/view/doi%3A10.18739%2FA2H35R; DOI:10.18739/A2H35R).

ORCID

Benjamin M. Jones https://orcid.org/0000-0002-1517-4711
Mikhail Kanevskiy https://orcid.org/0000-0003-0565-0187
Alexander Vasiliev https://orcid.org/0000-0001-5483-8456

REFERENCES

1. Sellmann PV. Geology of the USA CRREL permafrost tunnel, Fairbanks, Alaska. 1967. Hanover, New Hampshire, U.S. Army CRREL Technical Report 199.
2. Hamilton TD, Craig JL, Sellmann PV. The fox permafrost tunnel: a late Quaternary geologic record in Central Alaska. *Geol Soc Am Bull*. 1988;100(6):948-969.
3. Shur Y, French HM, Bray MT, Anderson D. Syngenetic permafrost growth: cryostratigraphic observations from the CRREL tunnel near Fairbanks, Alaska. *Permafr Periglac Process*. 2004;15(4):339-347.
4. French H, Shur Y. The principles of cryostratigraphy. *Earth Sci Rev*. 2010;110:190-206.
5. Bray MT, French HM, Shur Y. Further cryostratigraphic observations in the CRREL permafrost tunnel, fox, Alaska. *Permafr Periglac Process*. 2006;17(3):233-243.
6. Fortier D, Kanevskiy M, Shur Y. Genesis of reticulate-chaotic cryostructure in permafrost. In: Kane DL, Hinkel KM, eds. *Ninth International Conference on Permafrost*. Vol.1. Institute of Northern Engineering, University of Alaska Fairbanks; 2008:451-456.
7. Douglas TA, Fortier D, Shur Y, et al. Biogeochemical and geocryological characteristics of wedge and thermokarst-cave ice in the CRREL permafrost tunnel, Alaska. *Permafr Periglac Process*. 2011;22(2):120-128.
8. Shumskii PA. *Ground (subsurface) ice. Principles of geocryology, part I, general geocryology*. Moscow, Russia: Academy of Sciences of the USSR; 1959:274-327 Chapter IX. (in Russian) (English translation: C de Leuchtenberg), 1964. National Research.
9. Gasanov SS. *Structure and History of Formation of Permafrost in Eastern Chukotka*. Moscow: Nauka; 1969 (in Russian).
10. Mackay JR. Catastrophic lake drainage, Tuktoyaktuk Peninsula area, District of Mackenzie. In: *Current Research, Part D, Geological Survey of Canada, Paper*. Vol.88; 1988:83-90.
11. Mackay JR. A full-scale field experiment (1978–1995) on the growth of permafrost by means of lake drainage, western Arctic coast: a discussion of the method and some results. *Can J Earth Sci*. 1997;34(1):17-34.
12. Kanevskiy M, French H, Shur Y (Eds). Late-Pleistocene Syngenetic Permafrost in the CRREL Permafrost Tunnel, Fox, Alaska. In: *A guidebook prepared for Ninth International Conference on Permafrost*; 2008.
13. French HM. *The Periglacial environment*. 4thed. Chichester, UK: John Wiley and Sons ltd; 2018.
14. Kanevskiy M, Shur Y, Fortier D, Jorgenson MT, Stephani E. Cryostratigraphy of late Pleistocene syngenetic permafrost (yedoma) in northern Alaska, Itkillik River exposure. *Quatern Res*. 2011;75:584-596.
15. Schirrmeister L, Froese D, Tumskoy V, Grosse G, Wetterich S. Yedoma: Late Pleistocene Ice-Rich Syngenetic Permafrost of Beringia. In: *Encyclopedia of Quaternary Science (Second Edition)*; 2013:542-552.
16. Strauss J, Schirrmeister L, Grosse G, et al. Deep Yedoma permafrost: a synthesis of depositional characteristics and carbon vulnerability. *Earth Sci Rev*. 2017;172:75-86.
17. Ivanov MS. *Kriogennoe stroenie chetvertichnykh otlozheniy Leno-Aldanskoy vpadiny [Cryogenic structure of the Quaternary deposits of Lena-Aldan lowland]*. Novosibirsk, Russia: Nauka Press; 1984 (in Russian).
18. Romanovskii NN. *Osnovy kriogeneza litosfery [Fundamentals of cryogenesis of lithosphere]*. Moscow, Russia: Moscow University Press; 1993 (in Russian).
19. Fraser TA, Burn CR. On the nature and origin of "muck" deposits in the Klondike area, Yukon territory. *Can J Earth Sci*. 1997;34(10):1333-1344.
20. Kotler E, Burn CR. Cryostratigraphy of the Klondike "muck" deposits, westcentral Yukon territory. *Can J Earth Sci*. 2000;37(6):849-861.
21. Froese DG, Zazula GD, Westgate JA, et al. The Klondike goldfields and Pleistocene environments of Beringia. *GSA Today*. 2009;19(8):4-10.
22. Stephani E, Fortier D, Shur Y, Fortier R, Doré G. A geosystems approach to permafrost investigations for engineering applications, an example from a road stabilization experiment, Beaver Creek, Yukon, Canada. *Cold Reg Sci Technol*. 2014;100:20-35.
23. Fortier D, Strauss J, Sliger M, Calmels F, Froese D, Shur Y. Pleistocene yedoma in south-western Yukon (Canada): a remnant of Eastern Beringia? In: *5th European Conference on Permafrost – Book of Abstracts*; 2018:637-638.
24. Lawson DE. *Ground ice in perennially frozen sediments, northern Alaska. Proceedings of the Fourth International Conference on Permafrost*. Washington, DC: National Academy Press; 1983:695-700.
25. Lawson DE. Response of permafrost terrain to disturbance: a synthesis of observations from northern Alaska, USA. *Arctic Alpine Res*. 1986;18(1):1-17.
26. Carter LD. *Loess and deep thermokarst basins in Arctic Alaska. Proceedings of the Fifth International Conference on Permafrost*. Trondheim, Norway: Tapir Publishers; 1988:706-711.
27. Brewer MC, Carter LD, Glenn R. *Sudden drainage of a thaw lake on the Alaskan Arctic Coastal Plain. Proceedings of the Sixth International Conference on Permafrost*. Beijing, China: South China University of Technology Press; 1993:48-53.

28. Kanevskiy M, Shur Y, Strauss J, et al. Patterns and rates of riverbank erosion involving ice-rich permafrost (yedoma) in northern Alaska. *Geomorphology*. 2016;253:370-384.
29. Jorgenson MT, Kanevskiy M, Shur Y, Grunblatt J, Ping C-L, Michaelson G. Permafrost database development, characterization, and mapping for northern Alaska. 2014. Report for Arctic Landscape Conservation Cooperative by Alaska Ecoscience and University of Alaska Fairbanks.
30. Trochim ED, Schnabel WE, Kanevskiy M, Munk J, Shur Y. Geophysical and cryostratigraphic investigations for road design in northern Alaska. *Cold Reg Sci Technol*. 2016;131:24-38.
31. Gaglioti BV, Mann DH, Groves P, et al. Aeolian stratigraphy describes ice-age paleoenvironments in unglaciated Arctic Alaska. *Quat Sci Rev*. 2018;182:175-190.
32. Livingstone DA, Bryan K Jr, Leahy RG. Effects of an Arctic environment on the origin and development of freshwater lakes. *Limnol Oceanogr*. 1958;3(2):192-214.
33. Williams JR, Yeend WE. Deep thaw lake basins in the inner Arctic Coastal Plain, Alaska. In: *U.S. Geological Survey in Alaska: Accomplishments during 1978*; 1979 USGS Circular 804-B, B35-B37.
34. Farquharson LM, Mann DH, Grosse G, Jones BM, Romanovsky VE. Spatial distribution of thermokarst terrain in Arctic Alaska. *Geomorphology*. 2016;273:116-133.
35. Zimov SA, Davydov SP, Zimova GM, et al. Permafrost carbon: stock and decomposability of a globally significant carbon pool. *Geophys Res Lett*. 2006;33(20):L20502.
36. Kuhry P, Grosse G, Harden JW, et al. Characterisation of the permafrost carbon Pool. *Permafr Periglac Process*. 2013;24(2):146-155.
37. Strauss J, Schirrmeister L, Grosse G, et al. The deep permafrost carbon pool of the Yedoma region in Siberia and Alaska. *Geophys Res Lett*. 2013;40(23):6165-6170.
38. Fritz M, Opel T, Tanski G, et al. Dissolved organic carbon (DOC) in Arctic ground ice. *Cryosphere*. 2015;9(2):737-752.
39. Jorgenson MT, Brown J. Classification of the Alaskan Beaufort Sea coast and estimation of carbon and sediment inputs from coastal erosion. *Geo-Mar Lett*. 2005;25(2-3):69-80.
40. Grosse G, Harden J, Turetsky M, et al. Vulnerability of high-latitude soil organic carbon in North America to disturbance. *J Geophys Res*. 2011;116:G00K06.
41. Ping C-L, Michaelson GJ, Guo L, et al. Soil carbon and material fluxes across the eroding Alaska Beaufort Sea coastline. *J Geophys Res*. 2011;116:G02004.
42. Vonk JE, Mann PJ, Dowdy KL, et al. Dissolved organic carbon loss from Yedoma permafrost amplified by ice wedge thaw. *Environ Res Lett*. 2013;8(3):035023.
43. McClelland JW, Townsend-Small A, Holmes RM, et al. River export of nutrients and organic matter from the north slope of Alaska to the Beaufort Sea. *Water Resour Res*. 2014;50(2):1823-1839.
44. McClelland JW, Holmes RM, Peterson BJ, et al. Particulate organic carbon and nitrogen export from major Arctic rivers. *Global Biogeochem Cycles*. 2016;30(5):629-643.
45. Abbott BW, Jones JB, Godsey SE, Larouche JR, Bowden WB. Patterns and persistence of hydrologic carbon and nutrient export from collapsing upland permafrost. *Biogeosciences*. 2015;12(12):3725-3740.
46. Zhang X, Bianchi TS, Cui X, et al. Permafrost organic carbon mobilization from the watershed to the Colville River delta: evidence from ^{14}C ramped pyrolysis and lignin biomarkers. *Geophys Res Lett*. 2017;44(22):11,491-11,500.
47. Bristol EM, Connolly CT, Lorenson TD, et al. Geochemistry of coastal permafrost and erosion-driven organic matter fluxes to the Beaufort Sea near drew point, Alaska. *Front Earth Sci*. 2021;8:598933.
48. Fuchs M, Nitze I, Strauss J, et al. Rapid fluvio-thermal erosion of a yedoma permafrost cliff in the Lena River Delta. *Front Earth Sci*. 2020;8:336. https://doi.org/10.3389/feart.2020.00336
49. Morgenstern A, Overduin PP, Günther F, et al. Thermo-erosional valleys in Siberian ice-rich permafrost. *Permafr Periglac Process*. 2021;32:59-75.
50. Shur YL, Vasiliev AA, Veisman LI, Zaikanov VG, Maksimov VV, Petrukhin NP. Novye rezul'taty nablyudeniy za razrusheniem beregov v kriolitozone [New data of monitoring of shore erosion in permafrost region]. In: Are FE, ed. *Beregovye protsessy v kriolitozone [Shore processes in permafrost region]*. Novosibirsk, Russia: Nauka Press; 1984:12-19.
51. Shur Y, Vasiliev A, Kanevskiy M, Maksimov V, Pokrovsky S, Zaikanov V. Shore erosion in Russian Arctic. In: *Cold Region Impacts on Transportation and Infrastructure*. ASCE; 2002:736-747.
52. Aré FE. *Osnovy prognoza termoabrazii beregov [Fundamentals of forecast of thermal abrasion of shores]*. Moscow, Russia: Nauka Press; 1985 (in Russian).
53. Zaikanov V, Kanevskiy M. Beregovie protsessy v dolinakh krupnikh rek Severnoy Yakutii [The riverbank erosion in the valleys of large rivers in Northern Yakutia]. In: Grechishchev S, Vasiliev A, Sheshin Y, eds. *Metody izucheniya kriogennykh fiziko-geologicheskikh protsessov [Methods of study of cryogenic processes]*. Moscow: VSEGINGEO; 1992:16-29 (in Russian).
54. Zaikanov V, Kanevskiy M. Prichiny zagryazneniya Yany i Omoloya [the causes of contamination of the Yana and Omoloy Rivers]. *Priroda [Nature]*. 1992;9:90-94.(in Russian)
55. Grigoriev MN. Kriomorphogenez i litodinamika pribrezhno-shelfovoy zony morey Vostochnoy Sibiri [Cryomorphogenesis and lithodynamics of coastal-shelf zone of the seas of East Siberia]. Avtoreferat dissertatsii na soiskanie uchenoy stepeni doktora geograficheskikh nauk [synopsis of the doctor of science thesis]. 2008. Yakutsk (in Russian).
56. Stettner S, Beamish AL, Bartsch A, et al. Monitoring inter-and intra-seasonal dynamics of rapidly degrading ice-rich permafrost riverbanks in the Lena Delta with TerraSAR-X time series. *Remote Sens (Basel)*. 2018;10(1):51.
57. Grigoriev M, Rachold V. The degradation of coastal permafrost and the organic carbon balance of the Laptev and East Siberian Seas. In Proceedings of the 8th international conference on permafrost, 21–25 July 2003, Zurich, Switzerland, 2003;1: 319–324.
58. Günther F, Overduin PP, Sandakov AV, Grosse G, Grigoriev MN. Short- and long-term thermo-erosion of ice-rich permafrost coasts in the Laptev Sea region. *Biogeosciences*. 2013;10(6):4297-4318.
59. Williams JR. Effect of wind-generated waves on migration of the Yukon River in the Yukon flats, Alaska. *Science*. 1952;115(2993):519-520.
60. Walker HJ, Arnborg L. Permafrost and ice-wedge effect on riverbank erosion. In Proceedings of the International Conference on Permafrost, Lafayette, Indiana, 11–15 November 1963. Washington, DC: National Academy of Sciences—National Research Council, Publication 1287, 1966; 164–171.
61. Brice JC. Measurement of lateral erosion at proposed river crossing sites of the Alaska pipeline. U.S. Geological Survey Open-File Report 73–31, 1973.
62. Outhet DN. Bank erosion in the southern Mackenzie River Delta. M.S. thesis, University of Alberta, Edmonton, Alberta, 1974.
63. Scott KM. Effects of permafrost on Stream Channel behavior in Arctic Alaska. U.S. Geological Survey professional paper 1068. United States government printing office, Washington, 1978.
64. Walker J, Arnborg L, Peippo J. Riverbank erosion in the Colville Delta, Alaska. *Geogr Ann Ser B*. 1987;69(1):61-70.
65. Walker HJ, Jorgenson MT. Tour of the Colville River Delta. In: Jorgenson MT, ed. *Coastal region of northern Alaska. Guidebook to*

permafrost and related features. Alaska division of Geological & Geophysical Surveys guidebook 10, Part 4; 2011:85-135.
66. Stephani E, Jones B, Kanevskiy M. Assessing riverbank erosion and land cover changes in permafrost regions based on a terrain analysis approach, an example from the Colville River Delta, northern Alaska. 2019. In Proceedings of the 18th international conference on cold regions engineering and the 8th Canadian permafrost conference, Quebec City, Quebec, Canada, August 18–22, 2019: 678–686.
67. Porter C, Morin P, Howat I, Noh M-J, Bates B, Peterman K, Keesey S, Schlenk M, Gardiner J, Tomko K, Willis M, Kelleher C, Cloutier M, Husby E, Foga S, Nakamura H, Platson M, Wethington M Jr, Williamson C, Bauer G, Enos J, Arnold G, Kramer W, Becker P, Doshi A, D'Souza C, Cummens P, Laurier F, Bojesen M. ArcticDEM. 2020. https://doi.org/10.7910/DVN/OHHUKH, Harvard Dataverse, V1.
68. Strauss J, Shur Y, Kanevskiy M, et al. Expedition Alaskan North Slope/Itkillik 2012. In: Strauss J, Ulrich M, Buchhorn M, eds. *Expeditions to permafrost 2012: Alaskan north slope/Itkillik, Thermokarst in Central Yakutia, and EyeSight-NAAT-Alaska, Reports on Polar and Marine Research*. Vol.655. Bremerhaven, Germany: Alfred Wegener Institute for Polar and Marine Research; 2012:3-28.
69. Lapointe Elmrabti L, Talbot J, Fortier D, et al. Middle to late Wisconsinan climate and ecological changes in northern Alaska: evidences from the Itkillik River Yedoma. *Palaeogeogr Palaeoclimatol Palaeoecol*. 2017;485:906-916.
70. Jorgenson T, Yoshikawa K, Kanevskiy M, et al. Permafrost Characteristics of Alaska. In: Kane DL, Hinkel KM, eds. *Proceedings of the Ninth International Conference on Permafrost, extended abstracts*. Fairbanks, AK: Institute of Northern Engineering, University of Alaska Fairbanks; 2008:121-122.
71. Kane DL, Youcha EK, Stuefer SL, Myerchin-Tape G, Lamb E, Homan JW, Gieck RE, Schnabel WE, Toniolo H. Hydrology and meteorology of the central Alaskan Arctic: data collection and analysis. Final report. University of Alaska Fairbanks, water and Environmental Research Center, report INE/WERC 14.05, Fairbanks, AK, 2014.
72. Grosse G, Jones B, Schirrmeister L, Meyer H, Wetterich S, Strauss J, Gaglioti B, Mann DH, Romanovsky VE. Late Pleistocene and Holocene ice-rich permafrost in the Colville River valley, northern Alaska, PAST Gateways 2015, Potsdam, 18 May 2015-22 May 2015. Terra Nostra, 2015;1, 44–45.
73. Schirrmeister L, Dietze E, Matthes H, et al. The genesis of Yedoma ice complex permafrost – grain-size endmember modeling analysis from Siberia and Alaska. *E&G Quat Sci J*. 2020;69(1):33-53.
74. Mann DH, Groves P, Reanier RE, Kunz ML. Floodplains, permafrost, cottonwood trees, and peat: what happened the last time climate warmed suddenly in arctic Alaska? *Quat Sci Rev*. 2010;29(27-28):3812-3830.
75. Murton JB, Goslar T, Edwards ME, et al. Palaeoenvironmental interpretation of Yedoma silt (ice complex) deposition as cold-climate loess, Duvanny Yar, Northeast Siberia. *Permafr Periglac Process*. 2015;26(3):208-288.
76. Shur YL. On the transient layer. In: Shvetsov PF, Chistotinov LV, eds. *Methods of Geocryological Studies*. Moscow, Russia: USSR Institute of Hydrogeology and Engineering Geology; 1975:82-85 (in Russian).
77. Shur Y, Hinkel KM, Nelson FE. The transient layer: implications for geocryology and climate-change science. *Permafr Periglac Process*. 2005;16(1):5-18.
78. Shur YL. *Verkhniy gorizont tolshchi myorzlykh porod i termokarst [Upper horizon of permafrost and thermokarst]*. Novosibirsk, Russia: Nauka Press; 1988 (in Russian).
79. Kanevskiy M, Shur Y, Jorgenson MT, et al. Ground ice in the upper permafrost of the Beaufort Sea coast of Alaska. *Cold Reg Sci Technol*. 2013;85:56-70.
80. Rand J, Mello, M. Ice-coring augers for shallow depth sampling. 1985. CRREL Report 85–21.
81. van Everdingen RO (Ed). *Multi-Language Glossary of Permafrost and Related Ground-Ice Terms*. International Permafrost Association, University of Calgary; 1998 revised 2005.
82. Johnston GH. *Permafrost: Engineering Design and Construction*. Chichester, UK: John Wiley and Sons, Inc; 1981.
83. Himmelstoss EA, Henderson RE, Kratzmann MG, Farris AS. Digital Shoreline Analysis System (DSAS) version 5.0 user guide: U.S. Geological Survey Open-File Report 2018–1179. 2018.
84. Aré FE. Thermal abrasion of sea coasts (parts 1 and 2). *Polar Geogr Geol*. 1988;12(1 and 2):1-86.
85. Günther F, Overduin PP, Sandakov AV, Grosse G, Grigoriev MN. Thermo-erosion along the Yedoma Coast of the Buor-Khaya Peninsula, Laptev Sea, East Siberia. In: Hinkel KM, ed. *Proceedings of the Tenth International Conference on Permafrost, Salekhard, Yamal-Nenets Autonomous District, Russia*. Vol.1. International Contributions; 2012:137-142.
86. Kanevskiy M, Shur Y. 2015. Itkillik River data. Arctic data center. https://doi.org/10.18739/A2H35R
87. Shur Y, Osterkamp T. Thermokarst. Report INE 06.11. Fairbanks, AK: University of Alaska Fairbanks, Institute of Northern Engineering. 2007.
88. de Leffingwell E. Ground-ice wedges, the dominant form of ground-ice on the north coast of Alaska. *J Geol*. 1915;23(7):635-654.
89. Mackay JR. Segregated epigenetic ice and slumps in permafrost, Mackenzie delta area, N.W.T. *Geogr Bull*. 1966;8:59-80.
90. French HM. Active thermokarst processes, eastern Banks Island, Western Canadian Arctic. *Can J Earth Sci*. 1974;11(6):785-794.
91. Lewkowicz AG. Headwall retreat of ground-ice slumps, Banks Island, Northwest Territories. *Can J Earth Sci*. 1987;24(6):1077-1085.
92. Burn CR, Friele PA. Geomorphology, vegetation succession, soil characteristics and permafrost in retrogressive thaw slumps near Mayo, Yukon Territory. *Arctic*. 1989;42:31-40.
93. Burn CR, Lewkowicz AG. Retrogressive thaw slumps. *Can Geogr*. 1990;34(3):273-276.
94. Burn CR. The thermal regime of a retrogressive thaw slump near Mayo, Yukon territory. *Can J Earth Sci*. 2000;37(7):967-981.
95. Kokelj SV, Lantz TC, Kanigan J, Smith SL, Coutts R. Origin and polycyclic behaviour of tundra thaw slumps, Mackenzie Delta region, Northwest Territories, Canada. *Permafr Periglac Process*. 2009;20(2):173-184.
96. Lantz TC, Kokelj SV, Gergel SE, Henry GHR. Relative impacts of disturbance and temperature: persistent changes in microenvironment and vegetation in retrogressive thaw slumps. *Glob Chang Biol*. 2009;15(7):1664-1675.
97. Swanson DK, Hill K. Monitoring of retrogressive thaw slumps in the Arctic Network, 2010 baseline data: three-dimensional modeling with small-format aerial photographs. 2010. Natural Resource Data Series NPS/ARCN/NRDS—2010/123. Fort Collins, CO: National Park Service.
98. Swanson DK, Nolan M. Growth of retrogressive thaw slumps in the Noatak Valley, Alaska, 2010–2016, measured by airborne photogrammetry. *Remote Sens (Basel)*. 2018;10:983.
99. Stephani E, Kanevskiy M, Darrow M, Croft P, Drage J, Wuttig F. Early self-stabilization conditions of a retrogressive thaw slump, North Slope, Alaska. In: Deline P, Bodin X, Ravanel L, eds. *5th*

European Conference on Permafrost – Book of Abstracts; 2018: 207-208.
100. Zwieback S, Kokelj SV, Günther F, Boike J, Grosse G, Hajnsek I. Sub-seasonal thaw slump mass wasting is not consistently energy limited at the landscape scale. *The Cryosphere*. 2018;12(2): 549-564.
101. Shur YL, Vasiliev AA. Opyt izucheniya baydzharakhov na severe Yakutii [Study of baydzherakhs in Northern Yakutia]. In: Grechishchev SE, Chistotinov LV, Shur YL, eds. *Kriogennie protsessy [Cryogenic processes]*. Moscow, Russia: Nauka Press; 1978:220-233.
102. Aré FE. *Razrushenie beregov arkticheskikh primorskikh nizmennostey [Coastal erosion of the Arctic lowlands]*. Novosibirsk, Russia: Academic publishing house "geo"; 2012 (in Russian).

SUPPORTING INFORMATION

Additional supporting information may be found online in the Supporting Information section at the end of this article.

How to cite this article: Shur Y, Jones BM, Kanevskiy M, et al. Fluvio-thermal erosion and thermal denudation in the yedoma region of northern Alaska: Revisiting the Itkillik River exposure. *Permafrost and Periglac Process*. 2021;1–22. https://doi.org/10.1002/ppp.2105